ISTANBUL TECHNICAL UNIVERSITY ★ GRADUATE SCHOOL

MANUFACTURING AND CHARACTERIZATION OF POLYMER COMPOSITES BY USING SELECTIVE LASER SINTERING 3D PRINTING METHOD

Ph.D. THESIS

Burçin ÖZBAY

Department of Poymer Science and Technology

Poymer Science and Technology Programme

SEPTEMBER 2021

ISTANBUL TECHNICAL UNIVERSITY ★ GRADUATE SCHOOL

MANUFACTURING AND CHARACTERIZATION OF POLYMER COMPOSITES BY USING SELECTIVE LASER SINTERING 3D PRINTING METHOD

Ph.D. THESIS

Burçin ÖZBAY
(515152006)

Department of Poymer Science and Technology

Poymer Science and Technology Programme

Thesis Advisor: Prof. Dr. İ. Ersin SERHATLI

SEPTEMBER 2021

İSTANBUL TEKNİK ÜNİVERSİTESİ ★ LİSANSÜSTÜ EĞİTİM ENSTİTÜSÜ

SEÇİCİ LAZER SİNTERLEME 3D BASKI YÖNTEMİYLE POLİMER KOMPOZİTLERİN ÜRETİM VE KARAKTERİZASYONU

DOKTORA TEZİ

Burçin ÖZBAY
(515152006)

Polimer Bilim ve Teknolojisi

Polimer Bilim ve Teknolojisi Programı

Tez Danışmanı: Prof. Dr. İ. Ersin SERHATLI

EYLÜL 2021

Burçin ÖZBAY, a Ph.D. student of İTU Graduate School student ID 515152006, successfully defended the thesis/dissertation entitled "MANUFACTURING AND CHARACTERIZATION OF POLYMER COMPOSITES BY USING SELECTIVE LASER SINTERING 3D PRINTING METHOD", which she prepared after fulfilling the requirements specified in the associated legislations, before the jury whose signatures are below.

Thesis Advisor :	**Prof. Dr. İ. Ersin SERHATLI** İstanbul Technical University	.....
Jury Members :	**Prof. Dr. M. Hulusi ÖZKUL** Istanbul Technical University	.....
	Prof. Dr. Yusuf Z. MENCELOĞLU Sabancı University	.....
	Prof. Dr. H. Ayşen ÖNEN Istanbul Technical University	.....
	Assist. Prof. Dr. Nilüfer DUYGULU Yildiz Technical University	.....

Date of Submission : 26 August 2021
Date of Defense : 30 September 2021

To my precious family,

FOREWORD

This thesis was supported under 2211/C National Ph.D. Scholarship Program in the Priority Fields in Science and Technology. Firstly, I am thankful to TUBITAK for their support of my thesis research.

I would like to appreciate my supervisor Prof. Dr. Ersin SERHATLI, for his excellent guidance, valuable comments, and scientific support. I would also to thank my thesis committee members, Prof Dr. M. Hulusi ÖZKUL and Prof Dr. Yusuz Z. MENCELOĞLU, for their comments and recommendations throughout the thesis studies.

I wish to express my grateful thanks to Prof. Dr. Ahmet ÜNAL and Dr. Aylin ALTINBAY BEKEM for their support and for giving me an opportunity to use their polymer composite laboratory facilities during the experimental studies of my thesis.

I am also thankful to Dr. Ebubekir Koç and M. Enes BULDUK and my colleagues at Fatih Sultan Mehmet Vakif University, Aluminium Test, Training and Research Center (ALUTEAM).

I sincerely thank to my precious family for their encouragement and support during my academic studies and all my life. I will always be grateful to them.

Special thanks to Assoc. Prof. Dr. Alptekin KISASÖZ for his endless support, patience, and guidance.

September 2021

Burçin ÖZBAY
Metallurgical and Materials Engineer M.Sc.

TABLE OF CONTENTS

Page

FOREWORD ..... **ix**
TABLE OF CONTENTS ..... **xi**
ABBREVIATIONS ..... **xiii**
SYMBOLS ..... **xv**
LIST OF TABLES ..... **xvii**
LIST OF FIGURES ..... **xix**
SUMMARY ..... **xxi**
ÖZET ..... **xxiii**
1. INTRODUCTION **1**
1.1 Purpose of Thesis 3
1.2 Literature Review 3
1.3 Hypothesis 11
2. MATERIALS AND METHODS **13**
2.1 Materials 13
2.2 Processing Method 14
2.2.1 Processing of HGM filled PA 12 composites 16
2.2.2 Processing of different types of HGM filled PA 12 composites 17
2.2.3 Processing of different types of Cu filled PA 12 composites 17
2.2.4 Processing of flame retardant additive filled PA 12 composites 18
2.3 Characterization Methods 19
2.3.1 Powder characterizations 19
2.3.1.1 Particle size distribution 19
2.3.1.2 Microstructural analysis 19
2.3.1.3 Thermal analysis 19
2.3.2 Sintered sample characterizations 20
2.3.2.1 Mechanical tests 20
2.3.2.2 Density measurements 20
2.3.2.3 Microstructural analysis 20
2.3.2.4 Electrical conductivity test (4-point-probe method) 21
2.3.2.5 Flame retardancy tests 21
3. RESULTS AND DISCUSSION **23**
3.1 Properties of HGM Filled PA 12 Composites 23
3.1.1 Powder characterizations 23
3.1.1.1 Particle size distribution 23
3.1.1.2 SEM observations of powders 23
3.1.1.3 Thermal analysis 24
3.1.2 Sintered part characterizations 25
3.1.2.1 Mechanical test results and density measurements 25
3.1.2.2 SEM observations of sintered parts 29
3.2 Properties of Different Types of HGM Filled PA 12 Composites 29
3.2.1 Powder characterizations 29

3.2.1.1 Particle size distribution 29
3.2.1.2 SEM observations of powders 30
3.2.1.3 Thermal analysis 31
3.2.2 Sintered part characterizations 32
3.2.2.1 Mechanical test results and density measurements 32
3.2.2.2 SEM observations of sintered parts 36
3.3 Properties of Different Types of Cu Filled PA 12 Composites 40
3.3.1 Powder characterizations 40
3.3.1.1 Particle size distribution 40
3.3.1.2 SEM observations powders 40
3.3.1.3 Thermal analysis 41
3.3.2 Sintered part characterizations 43
3.3.2.1 Mechanical test results 43
3.3.2.2 SEM observations of sintered parts 46
3.3.2.3 Electrical test results (4-probe measuring method) 47
3.4 Properties of Flame Retardant Additive Filled PA 12 Composites 48
3.4.1 Powder characterizations 48
3.4.1.1 Particle size distribution 48
3.4.1.2 SEM observations of powders 49
3.4.1.3 Thermal analysis 50
3.4.2 Sintered part characterizations 50
3.4.2.1 Mechanical test results and density measurements 50
3.4.2.2 SEM observations of sintered parts 54
3.4.2.3 Flame retardancy test results of sintered parts 54
4. CONCLUSION 57
REFERENCES 59
CURRICULUM VITAE 65

ABBREVIATIONS

Al:	**:** Aluminium
AM	**:** Additive Manufacturing
B_2O_3	**:** Boron Oxide
CNTs	**:** Carbon Nanotubes
Cu:	**:** Copper
DSC	**:** Differential Scanning Calorimetry
DMA	**:** Dynamic Mechanical Analysis
FR	**:** Fire Retardant
H_3BO_3	**:** Boric acid
HGM	**:** Hollow Glass Microspheres
LS	**:** Laser Sintering
PA	**:** Polyamide
PA 6	**:** Polyamide 6
PA 11	**:** Polyamide 11
PA 12	**:** Polyamide 12
PE	**:** Polyethylene
PEEK	**:** Polyetheretherketone
PP	**:** Polypropylene
PS	**:** Polystyrene
SEM	**:** Scanning Electron Microscopy
SLS	**:** Selective Laser Sintering
TGA	**:** Thermogravimetric Analysis
TPU	**:** Thermoplastic Polyurethane

SYMBOLS

ED	**:** Energy Density
E'	**:** Storage Modulus
E''	**:** Loss Modulus
I	**:** Current
P	**:** Laser Power
ρs	**:** Sheet Resistance
Tg	**:** Glass Transition Temperature
Tm	**:** Melting temperature
Tβ	**:** β transition
v	**:** Laser Beam Speed (Laser Scan Speed)
V	**:** Voltage

LIST OF TABLES

Page

Table 2.1 : Materials Properties of polymer matrix and additives. **14**
Table 2.2 : Selective laser sintering process parameters. **16**
Table 2.3 : Selective laser sintering process parameters. **17**
Table 2.4 : Selective laser sintering process parameters. **18**
Table 2.5 : Selective laser sintering process parameters. **19**
Table 3.1 : DSC results:Melting and crystallization temperatures evaluation……...**24**
Table 3.2 : DSC results:Melting and crystallization temperatures evaluation……...**31**
Table 3.3 : DSC results:Melting and crystallization temperatures evaluations…….**42**
Table 3.4 : DMA data of PA 12 and Cu-filled PA 12 at T_β, 23ºC and T_g…….….**43**
Table 3.5 : DSC results:Melting and crystallization temperatures evaluations…….**50**
Table 3.6 : Flame retardancy test results of PA 12 and PA 12 composites……..….**55**

LIST OF FIGURES

Page

Figure 1.1 : The Additive Manufacturing Process Flow [2]. **1**
Figure 1.2 : a- Illustration of SLS Technique [17] b- Schematic representation of SLS [18]. **3**
Figure 1.3 : An illustration of AM principles for polymeric materials [21]. **4**
Figure 1.4 : Polymer Powder Consumption for Additive Manufacturing. **5**
Figure 1.5 : Thermogram with 'sintering window' as LS process temperature. **6**
Figure 1.6 : Worldwide flame retardants (FRs) market material categorization [44]. **10**
Figure 2.1 : SLS processing machine (left) , Rotary tumbler (right). **15**
Figure 3.1 : Volumetric particle distribution of a) PA 2200 (EOS), b) iM16K (3M) powders. **23**
Figure 3.2 : SEM images of powders of a) PA 2200 (EOS), b) iM16K (3M), c) 20% iM16K added PA 2200. ..... **24**
Figure 3.3 : TGA results of PA 12-10HGM, PA 12-15HGM, PA 12-20HGM. **25**
Figure 3.4 : Tensile test results. **26**
Figure 3.5 : 3 Point bending flexural test results. **27**
Figure 3.6 : Notched-Charpy impact test results. **28**
Figure 3.7 : Density measurement of sintered samples. **28**
Figure 3.8 : SEM images of sintered composite structures a) PA 12-10HGM-L-x1.00k, b) PA 12-15HGM- L-x1.00k, c) PA 12-15HGM-L-x500, d) PA 12 20HGM – L-x1.00k. **29**
Figure 3.9 : Volumetric particle distribution of a) PA 12, b) EHGMS-60S, c) HGB-M60, d) iM16k HGM, e) MWS-2575, f) EHGMS-60 powders. **30**
Figure 3.10 : SEM images of the polymer matrix and some of the additives (a)PA 2200 (EOS GmbH), b) iM16k HGM (3MTM), c) MWS 2575 (ELMINAS®)) **30**
Figure 3.11 : Tensile test results a) Maximum tensile stress, b) Maximum tensile strain. **33**
Figure 3.12 : Flexural test results a) Maximum flexural stress, b) Maximum flexural strain. **34**
Figure 3.13 : Notched Charpy impact test results. **35**
Figure 3.14 : Density measurements. **36**
Figure 3.15 : SEM observations of fracture surfaces after tensile test a) unfilled PA 12, b) PA12-20HGS60S, c) PA12-20HGB, d) PA12-20HGM, e) PA12-20MWS, f) PA12-20HGS60. ..... **37**
Figure 3.16 : SEM observations of fracture surfaces after impact test a) unfilled PA 12, b) PA12-20HGS60S, c) PA12-20HGB, d) PA12-20HGM, e) PA12-20MWS, f) PA12-20HGS60. ..... **39**
Figure 3.17 : Volumetric particle distribution of a) PA 12, b) Dendritic Cu powder, c) Spherical Cu powder. **40**

Figure 3.18 : SEM Images of a) Dendritic Cu, b) Spherical Cu, c) PA 12 polymer powders, d) PA 12-Dendritic Cu mixture, e) PA 12-Spherical Cu mixture. **41**
Figure 3.19 : TGA test results of PA12-S, PA12-D. **42**
Figure 3.20 : Flexural properties at various ED values a) Ultimate Stress b) Modulus. **45**
Figure 3.21 : Charpy impact test results. **46**
Figure 3.22 : SEM images of a), b) Dendritic Cu-filled sintered samples; c), d) Spherical Cu-filled sintered samples (the black arrows indicate copper reinforcements). **47**
Figure 3.23 : Conductivity values of PA 12 and Cu-filled PA 12 samples. **48**
Figure 3.24 : Volumetric particle distribution of a) PA 12, b) B_2O_3, c) Exolit-1230, d) Exolit 1400. ..... **49**
Figure 3.25 : SEM images of filler powders: a) B_2O_3, b) Exolit 1230, c) Exolit 1400. ..... **49**
Figure 3.26 : Tensile test results of a) PA 12-B_2O_3, b) PA 12-E-1230, c) PA 12-E-1400 composite structures. **51**
Figure 3.27 : Flexural test results of a) PA 12-B_2O_3, b) PA 12-E-1230, c) PA 12-E-1400 composite structures. **52**
Figure 3.28 : Charpy impact test results of a) PA 12-B_2O_3, b) PA 12-E-1230, c) PA 12-E-1400 composite structures. **53**
Figure 3.29 : Density measurements of a) PA 12-B_2O_3, b) PA 12-E-1230, c) PA 12-E-1400 composite structures. **53**
Figure 3.30 : SEM images of a) PA 12-B_2O_3, b) PA 12-E-1230, c) PA 12-E-1400 composite structures. **54**

MANUFACTURING AND CHARACTERIZATION OF POLYMER COMPOSITES BY USING SELECTIVE LASER SINTERING 3D PRINTING METHOD

SUMMARY

From the early invention of Additive Manufacturing (AM) from the 1960s to the 1990s, it has been rapidly developing worldwide within the last fifteen years. Studying this fast-growing technology has great importance for many application areas. Additionally, Selective Laser Sintering (SLS) is one of the improved methods of additive manufacturing and is crucial to develop thermoplastics and their composites. The thermoplastic material and thermoplastic matrix composite materials produced by this method have great potential to be used in the automotive and biomedical industries, aerospace and electric electronic sectors, and many others. In this area, hollow featured additives can be used to achieve lightweighted polymer composite structures. The density reduction is significant in enhancing fuel efficiency and reducing CO_2 emissions in the aerospace and automotive industries.

In the first part of the study, a Hollow Glass Microspheres (HGM) additive amount (10 wt. %, 15 wt. %, 20 wt. %) effects on Polyamide 12 (PA 12) polymer composite sintered parts as a means of the final density and mechanical properties of the composite structures were investigated. As the result of the study, the optimum HGM addition amount was detected as 20 wt. %.

After that the second part of the study has been started with the detected optimum amount of HGM addition to PA 12. The study aims to determine the effects of different types and the same amount of hollow featured additives on polyamide polymeric structures, which have been produced by SLS-AM technology. This part of the research covers the comparison of the same amount, and different types of Hollow Glass Microspheres (HGMs) filled Polyamide 12 (PA 12) polymer composites.

In the third part of the study, the metal additive effects on PA 12 polymer matrix were investigated. The electrical, thermal and mechanical effects of copper fillers on the PA 12 polymer matrix were examined. Two various types of Cu particles (spherical and dendritic) were introduced to the PA 12 polymer matrix in the same proportion (15 wt. %) as fillers. The thermal stability and thermal behaviors, crystallization kinetics, and heat capacities of copper-filled mixes and unfilled PA 12 were also analyzed. And the electrical conductivity of unfilled PA 12 and produced Cu-filled polymer composites were analyzed.

In the last part of the research, the flame retardancy properties of polymer composites that were produced by SLS, were investigated. Different types and the same amount of fire retardant additives were added to PA 12 polymer matrix. And unfilled PA 12 and produced polymer composites were analyzed in terms of mechanical characteristics and flame retardancy features.

For the SLS-AM processing EOS P 110 (EOS GmbH) SLS production machine with 100 microns of layer height was used in the study. To prepare polymer composite

powder mixtures, a rotary tumbler was used. For powder and sintered samples, material characterization tests were performed. All mechanical tests (tensile, 3 point bending, notched Charpy impact tests, and DMA) were performed according to the related ISO standards. On the other hand, the sintering window area detections were obtained by DSC graphs. They were used to determine optimum laser sintering process parameters, which are laser power, scan speed, and scan spacing.

SEÇİCİ LAZER SİNTERLEME 3D BASKI YÖNTEMİYLE POLİMER KOMPOZİTLERİN ÜRETİM VE KARAKTERİZASYONU

ÖZET

Eklemeli imalat 1960 ve 1990 arasında keşfedilmekle birlikte, son on beş yılda hızla gelişen ve dünya genelinde yaygın olarak kullanılan bir imalat yöntemidir. Bu yöntemde toz, reçine ya da filament şeklindeki başlangıç malzemesi, iki boyutlu tabakalar halinde katman katman imal edilerek üç boyutlu, belirli bir hacme ve dayanıma sahip nihai ürünler haline getirilir. Elde edilen nihai ürünler, geleneksel yöntemlerle üretilen ürünlerle kıyaslanabilecek üstün özelliklere sahiptir. Eklemeli imalat yönteminde iki boyutlu tabakalar arasında, üretim sırasında kurulan bağlar nihai ürünün oldukça iyi dayanım özelliklerine sahip olmasına neden olur. Bu bağların kurulmasında eklemeli imalatın temelini oluşuran sinterleme ve ergitme proseslerinin önemi vardır. Sinterleme ya da ergitme temelli proseslerde, ortaya çıkan enerji katmanlar arasında kuvvetli bağlar kurulmasını sağlar. Hızla gelişen bu teknolojinin incelenmesi birçok uygulama alanı için önem taşımaktadır.

Eklemeli imalatın, prosesin temelini oluşturan yönteme göre birçok çeşidi bulunmaktadır. Son yıllarda özellikle ergitme ve sinterleme temelli eklemeli imalat yöntemleri oldukça yaygın kullanılmaya başlanmıştır. Bu yöntemler arasında bulunan ve gelişmiş eklemeli üretim yöntemlerinden biri olan Seçici Laser Sinterleme (SLS), termoplastik polimer ve polimer kompozitlerin üretiminde kullanılmaktadır. Söz konusu yöntemde, hammadde toz şeklinde sisteme beslenir ve sıcaklık ve lazer yardımıyla sinterleme prosesi aktive edilip katmanlar arasında istenen bağlar kurularak üç boyutlu nihai ürünler elde edilir. Bu yöntemle üretilen termoplastikler ve termoplastik matrisli kompozitler otomotiv, biyomedikal, havacılık, elektrik ve elektronik gibi pek çok alanda büyük kullanım ve uygulama potansiyeline sahiptirler. Bu alanda, içi boş cam mikroküreler kullanılarak üretilen polimer matrisli kompozitlerle hafiflik sağlanabilir. Söz konusu ürünler havacılık ve otomotiv endüstrilerinde, yakıt verimliliğin artırılması ve CO_2 emisyonun azaltılması açısından, yapısal bileşenlerde ise hafifletme için oldukça önemlidir. Öte yandan kullanılacak farklı katkı maddeleri ile polimerlerin yanma geciktirme, elektirik iletkenliği gibi özellikleri de geliştirilebilir.

SLS yönteminin kompozit malzeme üretiminde kullanılması, uygun şekilde karıştırılmış polimer hammadde ve takviye tozlarının üretim sistemine beslenmesi ve uygulanan sıcaklık ve lazer prosesi ile birlikte kompozit malzeme üretimlerinin gerçekleşmesi şeklinde oluşmaktadır. Matris malzemesini oluşturan tozlar ile takviye elemanı olarak kullanılacak tozlar için sinterlenebilirlik özelliği ve tanecik boyutu gibi bazı sınırlandırmalar bulunmaktadır. Eklemeli imalat ile polimer kompozitlerin eldesinde, sinterleme penceresi oldukça önemli bir parametredir. Geniş sinterleme penceresine sahip olan polimerler, SLS yöntemiyle üretime daha yatkın

malzemelerdir. Bu nedenle poliamidler, özellikle Poliamid 12 (PA 12) eklemeli imalatta kullanılmaya oldukça uygun bir hammaddedir.

Bu çalışma eklemeli imalat ile PA 12 matrisli kompozit malzemelerin üretimine odaklanmıştır. Çalışma kapsamında farklı takviye malzemeleri kullanılarak PA 12 matrisli kompozit malzemelerin üretiminde hem eklemeli imalat prosesi parametreleri hem de üretilen nihai ürün özellikleri araştırılmıştır. Bu amaçla çalışma dört ana başlık altında yürütülmüştür.

Malzemelerin SLS yöntemiyle üretilmesinde EOS P 110 (EOS GmbH) cihazı kullanılmıştır. Polimer matrisli kompozitlerin karışımlarının hazırlanmasında döner karıştırıcı kullanılmıştır. Üretim sırasında her bir katman 100 mikron kalınlığa sahip olacak şekilde oluşturulmuştur ve sinterleme etkisi ile katmanlar arasında uygun bir bağ kuvveti kurulmasıyla, nihai ürünün üretimi sağlanmıştır. Kompozit malzeme üretiminde kullanılan tozlara ve sinterleme sonucunda elde edilen nihai ürünlere karakterizasyon testleri uygulanmıştır. Karakterizasyon testleri için öncelikle DSC analizleri ile sinterleme penceresi verisinden yola çıkılarak üretim sıcaklığı; lazer gücü, tarama hızı ve tarama aralığı gibi lazer verilerinin optimum değer aralıkları ve değerleri belirlenmiştir. Kompozit malzemelerin karakterizasyonunda ise mekanik ve fiziksel testler uygulanmıştır. Kompozit malzemelere uygulanan çekme ve eğme testleri ile hem dayanım değerleri belirlenmiş hem de uzama değerleri ortaya konmuştur. Charpy darbe deneyleriyle de malzemelerin kırılma anında sönümledikleri enerji değerleri araştırılmıştır. Böylece malzemelerin dayanım, uzama, darbe dayanımı gibi özellikleri belirlenmiştir. Öte yandan ilgili çalışmalarda üretilen kompozitlerin elektiriksel iletkenlik ve yanma geciktirme özellikleri de tespit edilmiştir. Uygulanan tüm testler uygun olan ISO ve ASTM standartlarına göre gerçekleştirilmiştir.

Çalışmanın ilk bölümünde, takviye malzemesi olarak kullanılacak olan içi boş cam mikroküreler farklı oranlarda (ağırlıkça %10, %15 ve %20) kullanılarak kompozit malzemeler üretilmiştir. Öncelikle PA 12 matris malzemesinin içi boş cam küreler ile takviye edilmesiyle, malzemenin sinterleme davranışı üzerindeki etkisi araştırılmıştır. Sonrasında ise içi boş cam küre takviyeli kompozit malzemeler üretilmiş ve yoğunluk değerleri ile mekanik özellikleri incelenmiştir. Yapılan incelemeler sonucunda ağırlıkça %20 oranında içi boş cam mikroküre içeren kompozit malzemenin optimum özelliklere sahip olduğu belirlenmiştir.

Çalışmanın ikinci bölümünde önceki kısımda belirlenen optimum içi boş cam mikroküre oranının farklı tür mikroküre katkıların kullanılmasıyla malzeme özellikleri üzerindeki etkisi araştırılmıştır. Seçilen farklı türdeki cam mikroküreler PA 12 matrisine katkılandırılmış ve cam mikrokürenin poliamid yapısına olan etkisi incelenmiştir. Kompozit malzeme içerisindeki takviye malzemesinin (içi boş cam mikroküre türü) malzeme özellikleri üzerinde etkisi olduğu belirlenmiştir. İçi boş cam mikroküre türünün değişmesiyle, özellikle kompozit malzemelerin sergiledikleri mekanik davranış değişmiş ve çekme dayanımı, eğme dayanımı, uzama ve darbe dayanımı gibi mekanik özellikler PA 12 matris malzemesine göre farklılaşmıştır. Sonuç olarak çalışmanın bu bölümünde farklı türdeki içi boş cam küre türlerinin aynı oranda kullanılmasıyla, içi boş cam mikroküre türünün PA 12 kompozit malzeme üzerindeki etkisi ortaya konulmuştur.

Çalışmanın üçüncü bölümünde, takviye malzemesi türünün değişmesiyle nihai ürün olan kompozit malzemenin özelliklerinin değişimi araştırılmıştır. Bu bölümde kompozit malzeme üretimi için PA 12 matrisi içerisine metal esaslı bakır katkılar ilave edilmiştir. Takviye malzemesi türü ve özellikleri, üretilecek kompozit malzeme

özellikleri açısından oldukça önemlidir. Metaller dayanım ve şekil değiştirme kabiliyetleri yüksek, ısı ve elektrik iletkenliği olan malzemelerdir. PA 12 matrisinin bakır ile katkılandırılması söz konusu özellikler açısından olumlu sonuçlar vermiştir. Metal katkının PA 12 matrisi üzerindeki etkisini daha iyi ortaya koymak amacıyla küresel ve dendritik morfolojiye sahip iki ayrı bakır toz ile çalışılmıştır. Böylece bakır toz morfolojisinin etkisi de detaylı olarak araştırılabilmiştir. Bakır katkılı kompozit malzemelerin üretiminde iki farklı türdeki katkı ağırlıkça %15 oranında PA 12 polimer yapısına ilave edilmiştir. Takviye oranının sabit bir değerde seçilmesiyle, bakır toz morfolojisinin etkisi üzerine yoğunlaşılmıştır. Bakırın yüksek ısıl ve elektriksel iletkenliği nedeniyle, PA 12 yapısının söz konusu özelliklerine odaklanılması elzem hale gelmiştir. Bu nedenle, PA 12 matris yapısının ve bakır katkılı kompozit malzemelerin elektriksel özellikleri, ısıl kararlılığı ve davranışı, kristalizasyon kinetiği ve ısı kapasitesi analiz edilmiştir.

Araştırmanın son bölümünde SLS ile üretilen polimer kompozitlerin alev geciktirici özellikleri incelenmiştir. PA 12 matrisli kompozit malzemelerin katkılandırılmasının mekanik özelliklerindeki değişimiyle birlikte, alev geciktirici özellikleri de önem kazanmaktadır. Mekanik özellik açısından teknik olarak kullanılabilecek bir PA 12 matrisli kompozitin, alev geciktirme özellikleri açısından takviye edilmemiş PA 12'ye alternatif bir malzeme olabilmesi için alev geciktirici özelliğinin de istenen kriter ve standartları sağlaması gerekmektedir. Bu amaçla son bölümde üretilen malzemelerin alev geciktirme özelliklerine odaklanılmıştır. PA 12 matris malzemesinin ve üretilen kompozit malzemelerin alev geciktirme özellikleri LOI ve UL-94 testleri ile analiz edilmiştir. Böylece alev geciktirme özelliği açısından da PA 12 matrisli kompozit malzemelerin özellikleri araştırılmıştır.

1. INTRODUCTION

Recently, Additive Manufacturing (AM), well known as three-dimensional (3D) printing, has been raised as an eco-friendly technology that provides energy saving, less material consumption, and efficient manufacturing [1]. Additive manufacturing, processing of small amounts of material at once, so that the successive parts to generate the desired fragment directly from a CAD model is a process that comprises adding to each other. Figure 1.1 shows the process steps of AM technology.

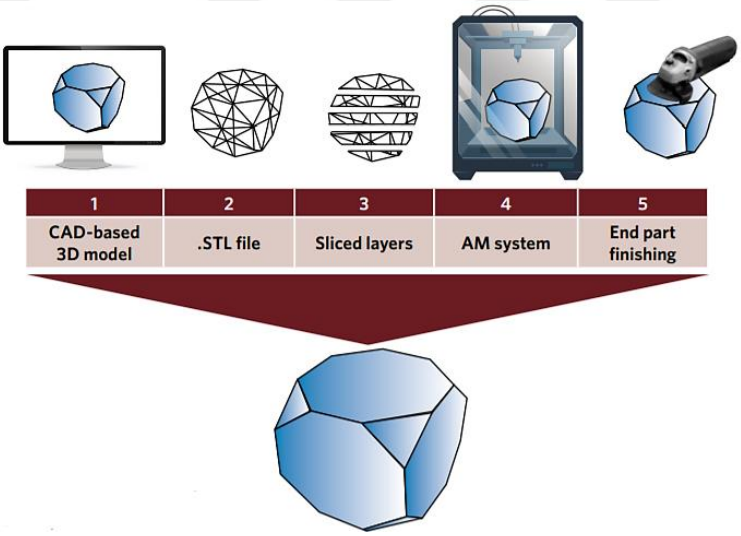

Figure 1.1 : The Additive Manufacturing Process Flow [2].

All 3D printing processes such as Fused Deposition Modeling (FDM), Stereolithography Apparatus (SLA), Selective Laser Sintering (SLS), Laminated Object Modeling (LOM) which stay in the additive manufacturing category as parts produced using the 3D printing process are made in one layer from the bottom up [3].

Additive manufacturing technology has the potential to penetrate a wide array of major industries from aerospace, automotive, consumer products to dental and medical products. Some of the main reasons why additive manufacturing is important in the rapid prototyping and manufacturing industry are apparent in its utilization [4, 5].

Selective laser sintering (SLS) is a powder-based additive manufacturing technology that uses the supplied energy by the laser to melt the polymer powders and then spread

the powder layer by layer to obtain target parts based on the 3D model data. A laser beam scans at an adjustable speed of the powder bed and coalescences the powder by complete melting or partial melting [6-8].

SLS was developed by Carl R. Deckard at University of Texas at Austin, USA, in 1980s. In 1987, it was commercialized by DTM Corporation, USA [1, 9]. SLS powder bed additive manufacturing systems contain a wide range of products (polymers, metals, ceramics). Polymer and polymer-based composites provide advantages such as low sintering energy consumption, good printing quality, high part accuracy, and easy post-SLS processing, etc. [4, 10, 11]. Although polymer, metal, and even ceramic materials can be processed, the heat sources that need high requirements while manufacturing causes obstacles to widespread usage of this technique [12].

When comparing 3D printing with traditional polymer manufacturing methods, like injection molding or extrusion, laser sintered parts are produced under pressure-free circumstances. The propellent power in laser sintering is the building chamber, and the temperature increase in the powder bed resulting from laser exposure. As a result of this, the properties of the manufactured parts correlate with energy input interaction and the melting temperature and the melting viscosity of the materials [13, 14].

In laser sintering, parts are built up layer by layer using layer thicknesses between 0.06 and 0.18 mm. This production method has three basic repeating stages for each layer. First of all, the platform descends an amount of up to one layer thickness. After that, a coater or a roller spreads the powder along the building platform, and the preheat set temperature is applied to the spread powder. Lastly, by laser scanner system CO_2-laser beam melts the powder. All these stages are repeated till the target parts are achieved [13, 15, 16]. In Figure 1.2 an illustration and schematic representation of SLS Technique can be seen.

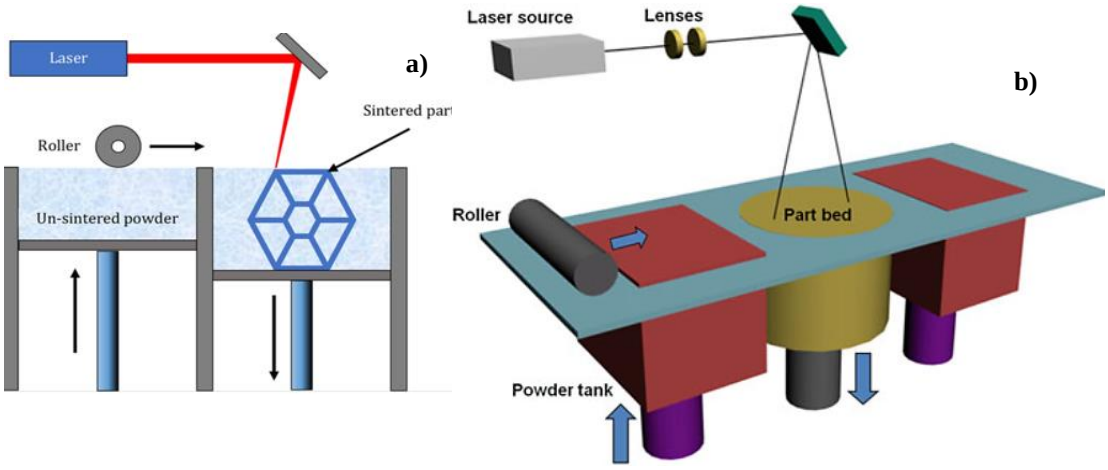

Figure 1.2 : a- Illustration of SLS Technique [17] b- Schematic representation of SLS [18].

1.1 Purpose of Thesis

The determination of process parameters and characterization of polymers and polymeric composite materials fabricated by one of the Additive Manufacturing (AM) methods is the Selective Laser Sintering (SLS) 3D printing method. The aim of the thesis is to study the mechanical properties, surface quality and geometric accuracy of laser sintered composites formed by the incorporation of additives in the polymer matrix. Additionally, the primary objectives of this research are as follows; to investigate the effect of filler type and amount and the content of the additive on the composite structure, to study the parameter settings and process optimization, and characterization of the sintered parts. Moreover, in terms of properties and quality, the main perspectives to be taken into consideration in Selective Laser Sintering (SLS) technology are the properties of the powders used in the process and the processing parameters for creating different types of additive filled polymer composites.

1.2 Literature Review

Additive Manufacturing (AM), is a manufacturing technique that implements the additive designing principle that constructs 3D geometries by addition of material layer by layer [19, 20]. Some other terms are also used to define AM process which are 3D printing, direct digital manufacturing, freeform fabrication, rapid prototyping, additive fabrication, additive layer manufacturing [21].

However, there are various types of additive manufacturing techniques for polymers. It is possible to process polymer materials in their powder, filament and sheet forms with this fabrication technique as well as some of AM technologies also use the active polymerization of photo-sensitive resins [17]. Figure 1.3 shows AM principles for polymeric materials in different forms.

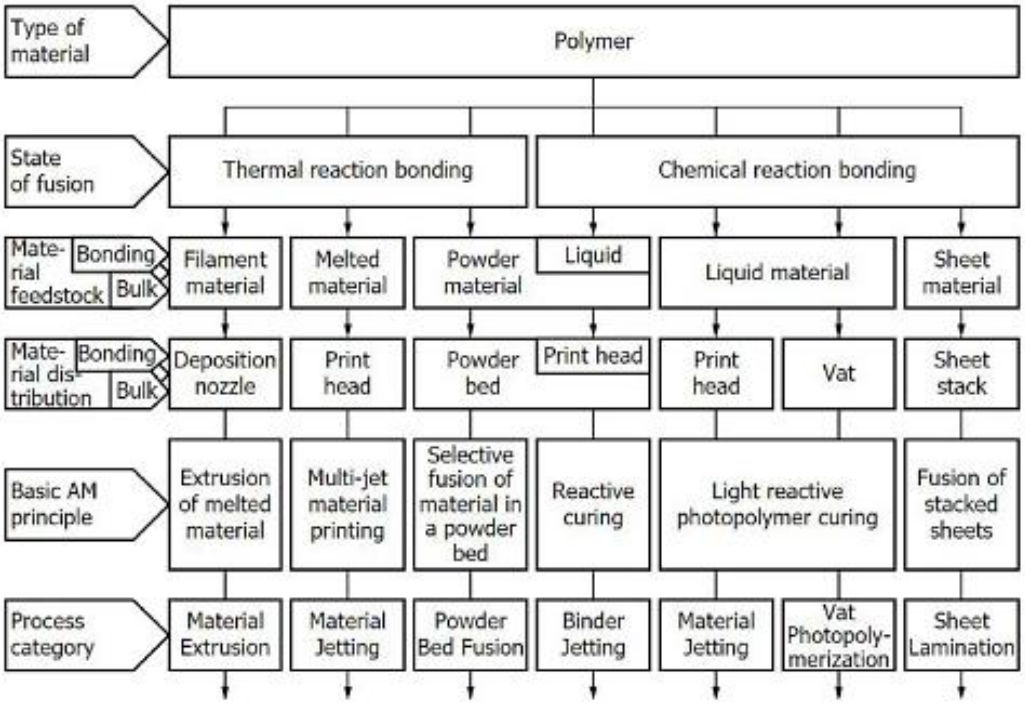

Figure 1. 3 : An illustration of AM principles for polymeric materials [21].

Although various materials, including polymer, ceramics, metal powders, and their composite powders, can be used in SLS, the polymers are more appropriate. Having relatively high viscosity in the liquid state and relatively low surface energy, exhibiting low reactivity with most gases, and having low thermal conductivity make polymers easy to process by SLS than other materials. To produce suitable products with SLS, the features of the powders that are used in manufacturing have to be taken into consideration. Thermoplastic polymers are well appropriate for SLS processing due to their comparatively low melting temperatures, low thermal conductivities, low agglomeration tendency, low sintering energy consumption, and good printing quality. However, the types of polymer materials developed in this field are mainly thermoplastic polymers, among which polyamide group materials [8, 22, 23].

Most common thermoplastic polymers for SLS is polyamides, Polyamide 12 (PA 12), Polyamide 11 (PA 11), and followed by Polyamide 6 (PA 6). There are also non-

polyamide laser sintering commercial materials such as Polypropylene (PP), Polyethylene (PE), Thermoplastic Polyurethane (TPU), Polyetheretherketone (PEEK), Polystyrene (PS), etc. [8, 21, 24, 25].

Significantly, the usage of polymer powder for AM technologies has been increasing day by day. Figure 1.4 shows global polymer powder consumption in the additive manufacturing industry between 2007-2019 [26].

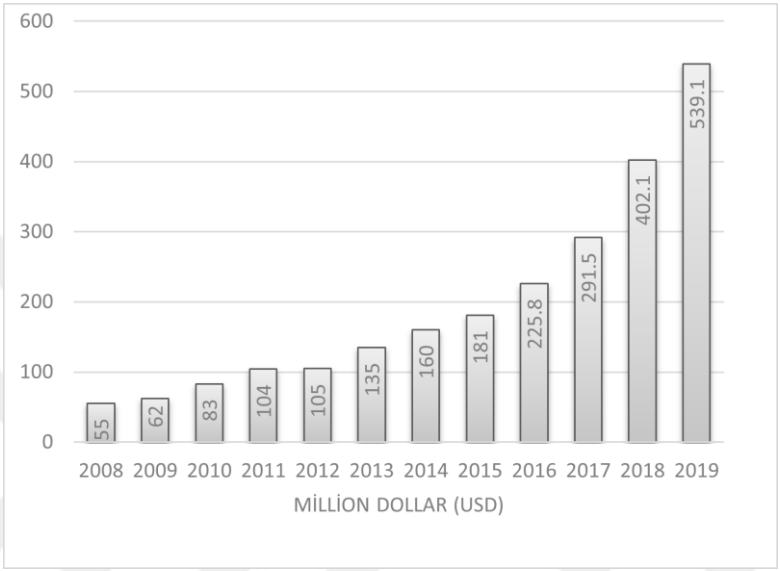

Figure 1.4 : Polymer Powder Consumption for Additive Manufacturing.

However, the sintering window is one of the most important criteria of consideration for the usability of a polymer powder in Laser Sintering (LS) process. The sintering window is between onset points of crystallization temperature and melting temperature. The DSC evaluation of powders ensures the temperatures which can be chosen in the process. Figure 1.5 [27] shows an example of a sintering window area in a DSC-Thermogram.

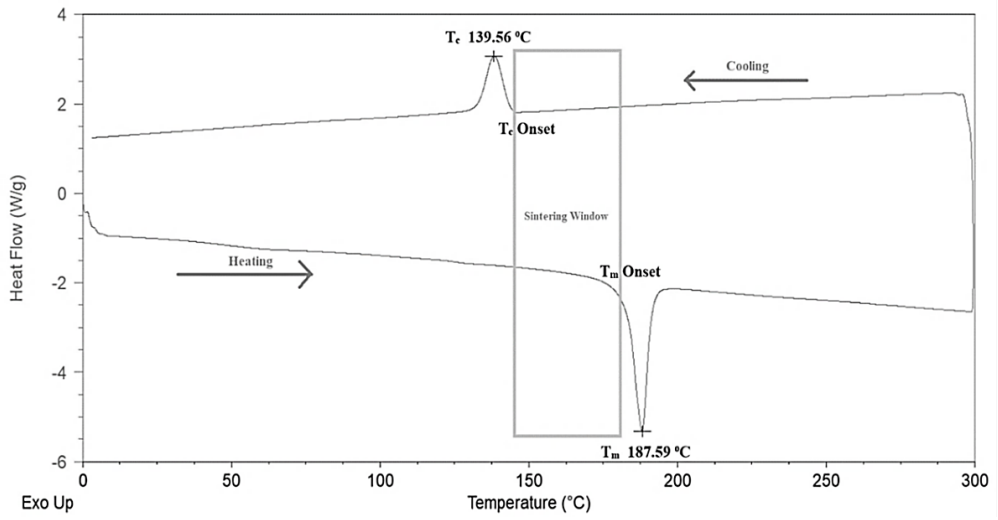

Figure 1.5 : Thermogram with 'sintering window' as LS process temperature.

Polyamides and Polyamide thermoplastic composites constitute 95% of the commercial market of PBF processes (SLS and multi-jet). Polyamide is not too sensitive to stress cracking, and at dry or low temperatures, it has excellent impact strength. Therefore, this material is desiring for rapid prototyping purposes and the most widely used material in SLS, producing parts with good long-term stability and also strength and durability [28-30].

Within the scope of this technology, the most used polymer material in powder bed additive manufacturing systems is Polyamide (PA) semi-crystalline thermoplastic polymers, primarily PA 12, followed by PA 11 and PA 6. The most widely known and used one, which is also used in this research, is PA 12. PA 12 is formed a combination of carbon atoms and amide group (COHN). PA 12 is a semi-crystalline polymer that includes both amorphous and crystalline structures [5, 31]. The chemical structure of PA 12 is given below:

$$[NH\,(CH_2)_{11}\,CO]_n \qquad (1.1)$$

Generally, the starting material in the production of commercial Polyamide 12 is laurolactam. Commercial production of Polyamide 12 is based on the ring-opening polymerization (Equ. 1.2 and 1.3) of laurolactam acid, amino acid or nylon salt can be used as catalysts, and these materials act as ring-opening reagents. Polyamide 12 can also be synthesis by an anionic polymerization mechanism using anhydrous alkaline catalysts [32, 33].

$$n[(CH_2)_{11}CONH] \rightarrow -[(CH_2)_{11}CONH]_n-$$

Laurolaktam Poliamid 12 (1.2)

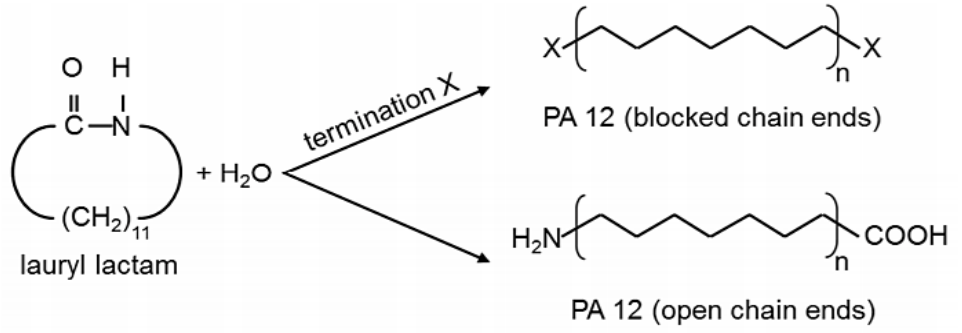

(1.3)

However, different types of micron and nano-level fillers, such as glass beads, silica, graphene, carbon nanotube (CNTs), carbon black, aluminum (Al), and copper (Cu), can be added to polymers to enhance their thermal, electrical, and mechanical properties [28, 34-36].

Mousa [34], has studied the surface modification and the filler amounts' effect on mechanical properties of SLS Polyamide 12 composites. Various mechanical properties, such as tensile strength, elasticity modulus, elongation at break, flexural strength and modulus, impact strength, fracture toughness and microstructural properties of PA 12-Glass Beads composites, were examined in this research. Regarding the mechanical test results, it can be inferred that by addition of glass beads with the ratio of 10%, 20%, 30%, 40% (two different types of glass beads) to Polyamide 12 improves the tensile strength and elastic modulus and decreases the impact strength and ductility of the sintered composite parts.

Negi et al. [25] studied the SLS process for flexural strength improvement of glass bead-filled PA12 (PA-3200 GF from the EOS GmbH). Also, ANOVA, which is a mathematical model, was utilized to estimate the flexural strength of laser-sintered PA 3200GF parts. The primary purpose of the research was to determine the process parameters' effects which are part bed temperature, laser power, scan speed, and scan spacing, on the flexural strength of produced parts. The modeling and observations showed the maximum flexural strength under optimized sintering conditions of 178 °C part bed temperature with 36 watts laser power, 2500mm/s scan speed, and 0.25mm scan spacing.

Wudy et al. [37] were studied the effect of amount and type filler as well as manufacturing parameters at Selective Laser Sintering. They did composite with different amount and types of glass bead additives. The characterization was performed basically about the evaluation of bulk densities and to detected material behavior optically and thermally. According to observations, by the addition of glass spheres, the bulk density of the final parts was increased. It is also found that while the glass content increased, crystallization temperature increased as well. Therefore, undesirable curling was observed during the processing. Additionally, they could decrease diffuse reflectance by increasing the filler amount in the mixture.

Cano et al. [38] investigated the effects of the orientation and the temperature on the mechanical properties of unfilled and GB filled PA 12. PA2200 as neat PA12 and PA3200 as 40% wt of glass beads reinforced PA 12 were used. It was specified that performing tensile and fracture tests at different temperatures via applying the load perpendicular and parallel. As a result, it has been observed that PA 12 had elevated fracture resistance than glass bead-filled PA12 composite. The weak interfacial connection between glass beads and the polymer matrix was defined as the reason for this result. Besides, there is an increase in the Young's modulus and tensile strength with decreasing temperature. Conversely, a decrease was observed for the Poisson's ratio and the elongation at break.

Chung et al. [39] investigated the manufacturing and properties of glass bead-filled with different volume fractions (0–30%) Nylon-11 composites. This research was a combination of experimental studies, theoretical modeling and numerical analysis. They performed tensile and compressive tests and then compared them with the results which estimated by a theoretical model. They were obtained good agreement between experimental results and the theoretical model. The tensile and compressive modulus were developed while strain at break and strain at yield decreases by increasing GB volume fraction.

Athreya et al. [40] investigated SLS manufacturing, and characterization of 4 wt.% filled carbon black (CB) Nylon-12 nanocomposite. It can be said that according to conducted tests CB filled nanocomposite structures had five orders of magnitude higher electrical conductivity ($1\times10-4$ S/cm) than the neat polymer processed by SLS. However, there was a decrease observed at flexural modulus from 1750MPa to

1450MPa. The authors explained the reason as a segregation occurrence in the nanocomposite structure which may be caused by poor matrix-filler interface.

Athreya et al. [41] were investigated the mechanical and microstructural properties of Nylon-12/carbon black composites, which SLS manufactured, melt compounding and injection molding (Extrusion-Injection Molding (Ex-IM)). According to the mechanical test results, the composites which were fabricated by SLS showed higher flexural and tensile modulus than Ex-IM manufactured composites. However, the mechanical properties of Carbon Black (CB) filled PA SLS parts had lower values than unfilled PA SLS parts. Because of the insufficient dispersion of nano-level CB and high porosity of the composites which were produced by SLS were presented as possible reasons by authors.

Jing et al. [42] were investigated how is the effects of the surface modification and reinforcing amount in carbon fiber (CF)/nylon 12 (PA12) composites of CFs while processing by selective laser sintering (SLS). Surface modification of CFs was conducted by nitric acid (HNO_3); after that SEM, FT-IR and XPS observations were performed. According to mechanical test results, there was an increase observed as 11% and 5% for the tensile strength and tensile modulus, respectively; and and the bending strength and bending modulus were improved by 7% and 11%, respectively, when compared with unmodified CF/PA12 sintered parts. Besides, HNO_3 modified CFs has oxygen functional groups on their surfaces which was resulted in partly thermal decomposition and released as gas in the SLS process which resulted as a high porosity and poor mechanical properties of the sintered specimens. To avoid this problem, they were performed a treatment at 400 °C under N_2 protection to HNO_3 treated CFs. As a result, the laser sintered parts had low porosity.

However, improving the flame retardancy properties of the polymer is a significant issue. Fire retardant polymers and polymeric composites, which are an essential and mandatory requirement for the aviation industry, are among the features that have been tried to be added to the material with the products produced by additive manufacturing.

The biggest part of the FR market includes minerals: metallic hydroxides, hydroxycarbonates, inert fillers, etc. Boron-based FRs present another family of inorganic flame-retardant additives: zinc borates, boric acid (H_3BO_3), and boron oxide (B_2O_3). On the other hand, the fastest-growing market is phosphorus-based FR

additives due to the lack of toxicity compared to halogenated FRs [43]. Figure 1.6 illustrates global flame retardant material consumption.

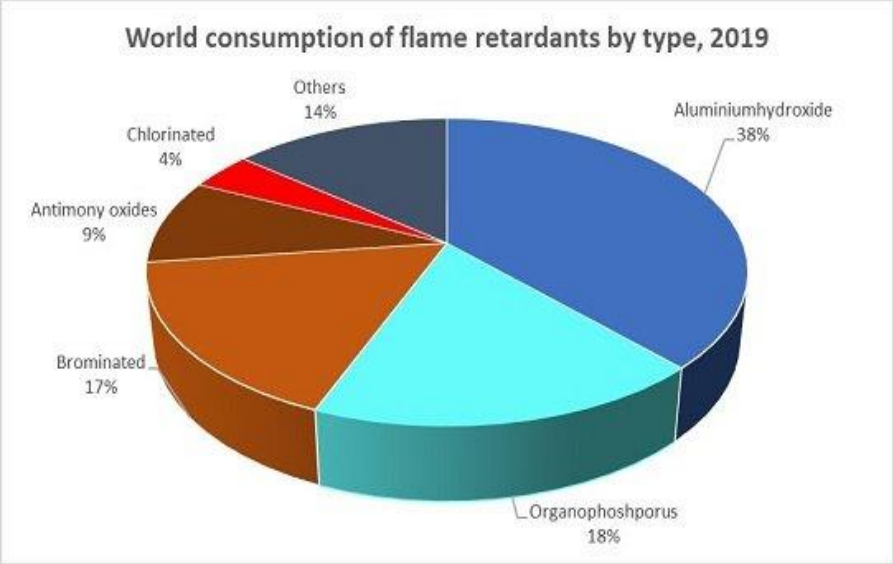

Figure 1.6 : Worldwide flame retardants (FRs) market material categorization [44].

Engineering polymers are often used as fossil fuels. It is highly flammable because it is produced from hydrocarbon-based raw materials. Nano additives such as nanoclays, nanosilica and polyhedral oligomeric silsesquioxane to enhance the flame retardant performance of polymers. There are some studies on the use of flame retardant additives such as phosphorus/nitrogen-based compounds [28]. However, only a few studies on the influence of additives on fire behavior for laser-sintered parts have been published.

Koo et al. [10] to add flame retardant properties to 70% PA 11 They added 10% flame retardant additive, 15% elastomer (Kraton), and 5% nanoclay, each by weight, and tried different formulations with the same amount of Kraton. All mixtures were prepared by the melt method, and then the granules were reduced to micron sizes by cryogenic crushing, and test samples were produced in the SLS method. According to the test results, longer burning times were observed in all products except for a single formulation (62.5% PA 11+20% FR additive+10% Kraton+7.5% Nanoclay).

Batistella et al. [45] were used ammonium polyphosphate (Exolit® AP422 and AP423-Clariant), phosphinate (Exolit® OP950), melamine polyphosphate (Melapur® 200 Basf), cyanurate melamine (Melapur® MC50-Basf), and Aflammit® PCO900 (Thor) as flame retardants to PA 12 (PA2200, EOS). As a result of cone calorimeter tests, the addition of flame retardants provided improved flame retardancy features of SLS

manufactured parts. Also, it was inferred that leading to a decrease in heat release peak, which is a function of the flame retardant type and loading.

Schneider et al. [46] investigated the flame-retardant properties of SLS produced PA 12 composites. In the study, two different types of phosphinate-based fillers (Exolit 1230, Exolit 1400)were used with various amounts (10, 12, 15, 18, 20, and 25 wt.%). Exolit 1230 demonstrated advanced flame retardancy features with a V-1 UL-94 rating for a concentration of 25 wt.%, while the sintered samples with 12, 15, 18, and 20 wt.% of filler added ones showed V-2 UL-94 rating. Besides, LOI values were higher Exolit 1230 with the increasing amount of flame retardant.

It is possible to create lightweigted SLS-produced structures by the addition of hollow features additives. Regarding past researches, there are studies about glass beads filled polymeric materials in SLS. However, the production of lightweight SLS parts, which are filled with

HGM particles have not been under detailed investigation. Therefore, a part of this research has been built on observing hollow featured additives' physical and mechanical effects on polymer composite structures. On the other hand, little researches have been done to examine the effects of metal additives on SLS manufactured polymeric structures. Besides, there are not much research has been conducted to a detailed examination of the integration of the thermal, electrical, and mechanical characteristics of metal-added SLS manufactured polymer composites. Nevertheless, flame retardant additive filled PA 12 polymer composite structure.

1.3 Hypothesis

Additive manufacturing technology has the possibility to penetrate lots of major industries from aerospace, automotive, consumer products to dental and medical products. It can be seen as follows some of the main reasons why additive manufacturing is important in the rapid prototyping and manufacturing industry as well. Flexible and lightweight component manufacturing with hollow or lattice structures can be produced, direct manufacturing can be done as components to their final or close to their final shape with minimum or no additional processing need, which means there is no additional tooling or manufacturing cost. Therefore, creating

new types of polymer composite materials and to improve existing ones with this recent technology is of significant importance.

Determination of process parameters and characterization of polymers and polymeric composite materials which are fabricated by one of the Additive Manufacturing (AM) method which is Selective Laser Sintering (SLS) 3D printing method. The aim of the thesis is to study the physical and mechanical properties, surface quality and geometric accuracy of laser sintered composites formed by the incorporation of additives in polymer matrix. Additionally, the primary objectives of this research are as follows; to investigate the effect of filler type and amount and the content of the additive on the composite structure, to study the parameter settings and process optimization, to characterize of the sintered parts. Moreover, in the way of properties and quality, the main perspectives to be taken into consideration in Selective Laser Sintering (SLS) technology are the properties of the powders used in the process and the processing parameters.

In this technology, one of the most important question is how can the features of polymer matrix improve by using additives. According to consideration around this question, it is possible to use different kind of fillers such as hollow glass beads, metals, silica, glass beads, some other nano or micro level additives or combinations of them. Secondly, it is also important to reseach interface compatibility between matrix and additives and how this improvement will result in as physical and mechanical properties of the final produced structure. However, the geometric accuracy of SLS sintered parts can be provided by managing the materials' properties. Therefore, it is vital that to detect the optimal conditions for manufacturing parameters as well. According to literature review, although many composite materials have been studied in this area, how the results will be for the use of many additives and combinations thereof are not known yet. E.g. it is possible to study for the purpose of from weight reduction to flame retardancy in different topics. Hence, this area can be considered to be a very suitable field for new research studies. As a result in the scope of the thesis, lightweight polymer composites would be developed for aerospace and automotive industries.

2. MATERIALS AND METHODS

2.1 Materials

This study has been conducted under three different scopes: providing lightweighting with hollow featured additives; investigating the electrical properties of metal added PA 12 polymer composites; and advancing flammability properties of PA 12 by the addition of flame retardant additives.

The main polymer matrix was Polyamide 12 that is PA2200 from EOS GmbH. The bulk density of EOS PA 2200 sintered parts is 0.93 g/cm^3 [47].

First of all, for the lightweigting part of the study, hollow featured additives were used. For this purpose, different kinds of Hollow Glass Microspheres (HGMs) were used. Used HGMs are iM16k HGM from 3M™ Company; EHGMS-60S, EHGMS-60, HGB-M60, MWS-2575 from ELMINAS®. Table 2.1 shows the information on polymer matrix and used additives.

Secondly, different types of copper (Cu) additives were used to investigate the electrical and mechanical effects of Cu additive on PA 12 polymer matrix. Dendritic-shaped Cu powders and spherical Cu powders were supplied from Merck and Nanografi, respectively.

Finally, different types of additives were used to improve the flammability properties of PA 12 polymer matrix to produce polymer composites. B_2O_3, Exolit® OP 1230, Exolit® OP 1400 were used as halogen-free additives to improve the flame retardant property of PA 12 polymer matrix. B_2O_3, and Exolit® OP 1230-Exolit® OP 1400 were supplied from Nanokar and Clariant, respectively.

Table 2.1 : Materials Properties of polymer matrix and additives.

Additive	Composition Information	True Density (g/cm^3)	Average Particle Size (D50) (μm)	Crush Strength (MPa)
PA 2200	Unfilled Polyamide 12	0.45	60.00	–
EHGMS-60S	SiO_2: 57-88; NaO_2: 8-16; CaO: 4-12; B_2O_3: 15-19; Other: 10-20	0.60	55.00	55.20
HGB-M60	SiO_2: 50-80; NaO_2: 7-20; CaO: 8-25; B_2O_3: 7-20	0.58–0.65	45.00	82.00
iM16k HGM	Soda-lime-borosilicate glass	0.46	23.50	110.00
MWS-2575	inorganic spherical elements-rod shaped acicular mineral elements	0.70	61.50	–
EHGMS-60	SiO_2: 57-88; NaO_2: 8-16; CaO: 4-12; B_2O_3: 15-19; Other: 10-20	0.60	30.50	68.90
Dendrtic Copper	99.99 % purity	8.9	63.00	–
Spherical Copper	99.99 % purity	8.9	90.00	–
Boron Oxide	99.9 % purity B_2O_3	1.10	44.00	–
Exolit 1230	Non-halogenated Highly stable phosphinated	1.35	35.00	–
Exolit 1400	Non-halogenated Highly stable phosphinated	1.40	45.00	–

2.2 Processing Method

The additive manufacturing machine (3D Printer) is FORMIGA P 110 Velocis from EOS Company. The Laser type is CO_2, 30 W. Its dimensions (WxDxH) are 1320x1067x2204 mm^3. For the preparation of the composite, a dry mechanical mixing method was used, and composite mixtures were prepared by a rotary tumbler (Figure 2.1).

Figure 2.1 : SLS processing machine (left) , Rotary tumbler (right).

For the SLS production by EOS FORMIGA P 110 Velocis machnine, the layer height can be used between 60-120 microns. In this study, 100 microns of layer height was applied. Under ISO and ASTM international test standards (according to different purposes; tensile, flexural, notched charpy impact, DMA, UL-94, and oxygen index tests), test specimens were produced from neat PA 12, and filled PA 12 polymer composites.

To obtain optimum laser sintering process parameters, different temperatures, in which sintering window range, were tried with different laser power, scan speed, and hatch distance (scan spacing) values. For Energy Density (ED) calculations below formula (Equ. 2.1) [48] was used. Where ED, P, v, h is energy density (J/mm^2), laser power (W), laser beam speed (mm/s), scan spacing or hatch distance (mm), respectively.

$$ED = \frac{V}{P\,h} \tag{2.1}$$

And then, the optimal processing temperatures and the process parameters were determined for each different composition. It was vital to create and detect which additives will be added to the polymer matrix and with which amounts to make experimental studies and appropriate processing parameters determination for SLS productions. Detailed material characterization and process temperature

determination were done for all productions by thermal and microstructural analysis of powders and production trials. As explained in detail in the powder characterization parts of the sections, DSC analysis was done to detect the sintering window area, crystallization, and melting temperatures of all mixtures and unfilled PA 12 itself. With the addition of the fillers, crystallization temperatures increased. For some additives, it has been shifted to higher temperatures. This situation may result in changing the processing parameters.

The fillers act as a nucleus, while the crystallization temperature is reached to higher temperatures. Therefore, it will be necessary to apply higher energy density values and processing temperatures [25, 27, 49, 50]. Thus, higher energy densities and temperatures were performed.

2.2.1 Processing of HGM filled PA 12 composites

As mentioned above, after several trials with changing laser processing parameters (energy density (J/mm^3), laser power (W), hatch distance (mm), optimum processing parameters were obtained. Test samples were produced with optimum temperature, and processing parameters for Hollow Glass Microsphere (HGM) filled composites. 170 °C is the processing temperature for neat PA 12. 176 °C is the optimum processing temperature for PA 12-10HGM, PA 12-15HGM, and PA 12-20HGM composite structures. PA 12-10HGM, PA 12-15HGM, and PA 12-20HGM represent 10%, 15%, and 20% of HGM filled PA 12 composite structures, respectively. Table 2.2 demonstrates SLS optimum process parameters of neat polymer and filled ones.

Table 2.2 : Selective laser sintering process parameters.

Material	Filler Content (%)	Building Chamber Temperature (°C)	Laser Power (mm/s)	Scan Speed (mm/s)	Hatch Distance (mm)	Energy Density (ED) (J/mm^3)
PA 12	0	170	21	2500.0	0.25	0.336
PA 12-10HGM	10	176	21	2187.0	0.25	0.384
PA 12-15HGM	15	176	21	1950.0	0.25	0.430
PA 12-20HGM	20	176	21	1787.5	0.25	0.470

2.2.2 Processing of different types of HGM filled PA 12 composites

From the first processing characterizations of HGM, 20% of HGM addition was defined as the optimum HGM filler amount. Therefore, different types of hollow features additives were supplied and the same amount (20%) filled to PA 12 polymer matrix. To determine optimum process parameters, several trials (different processing parameter sets) were performed. The optimal processing temperatures and the process parameters were detected for all compositions. After determining the optimum LS processing parameters, the test samples were prepared. Table 2.3 exhibits SLS optimum process parameters of neat polymer and 20% and different types of HGM filled polymer composites.

PA 12-20HGS60S, PA 12-20HGB, PA 12-20HGM, PA 12-20MWS, PA 12-20HGS60 represent 20% of EHGMS-60S, HGB-M60, iM16k HGM, MWS-2575, EHGMS-60, filled polymer composite structures, respectively.

Table 2.3 : Selective laser sintering process parameters.

Material	Filler Content (%)	Building Chamber Temperature (°C)	Laser Power (W)	Scan Speed (mm/s)	Hatch Distance (mm)	Energy Density (ED) (J/mm^3)
PA 12	0	170	21	2500	0.25	0.336
PA 12-20HGS60S	20	170	21	2000	0.25	0.420
PA 12-20HGB	20	172	21	1800	0.25	0.460
PA 12-20HGM	20	176	21	1787	0.25	0.470
PA 12-20MWS	20	178	21	1600	0.25	0.520
PA 12-20HGS60	20	178	21	1575	0.25	0.530

2.2.3 Processing of different types of Cu filled PA 12 composites

To produce the polymer composite mixtures at 15 wt. % Cu, a rotary tumbler at 30 rpm for 100 minutes was performed. PA12-S and PA12-D represent the spherical and dendritic copper-filled polymer composite structures, respectively.

The SLS process was carried out on an EOS P 110 (EOS GmbH) machine with 100 microns of layer height. For the manufacturing of neat PA 12, default parameters (21 W laser power, 2100 mm/s laser beam speed, and 0.25 mm scan spacing) were used at 170 ℃. The production of dendritic and spherical copper-filled PA 12 polymer composites with SLS was carried out at different energy densities in the range of 0.42

J/mm^3-0.47 J/mm^3. Laser scanning speed and scan spacing were fixed at 1900 mm/s and 0.20 mm, respectively. The temperature was kept constant at 173 ℃ in all copper-added productions. The production was initially attempted at 170 ℃, which is the optimal production temperature for neat PA 12, but after a few layers, a severe curling problem was noted, particularly at the edges of the samples. As a result, the temperature was raised in 1 ℃ steps until 173 ℃ was discovered as the optimal processing temperature for Cu-filled composites. Processing parameters can be seen in Table 2.4.

PA 12-D and PA 12-S represent 15 wt. % of dendritic and spherical copper filled PA 12 polymer composite structures, respectively.

Table 2.4 : Selective laser sintering process parameters.

Material	Filler Content (%)	Building Chamber Temperature (°C)	Laser Power (W)	Scan Speed (mm/s)	Hatch Distance (mm)	Energy Density (ED) (J/mm^3)
PA 12	0	170	21	2500	0.25	0.336
PA 12-D/S	15	173	21	0.20	0.20	0.420
PA 12-D/S	15	173	21	0.20	0.20	0.430
PA 12-D/S	15	173	21	0.20	0.20	0.440
PA 12-D/S	15	173	21	0.20	0.20	0.460
PA 12-D/S	15	173	21	0.20	0.20	0.470

2.2.4 Processing of flame retardant additive filled PA 12 composites

As applied in the previous mentioned studies, after several trials with changing laser processing parameters (energy density (J/mm^3), laser power (W), hatch distance (mm), and processing temperatures, optimum processing parameters were obtained. 170 °C is the processing temperature for neat PA 12, which was produced by default parameters. However, 173 ℃ is the optimum processing temperature for 7.5 wt. % of PA 12-B_2O_3, PA 12-E-1230, PA 12-E-1400 filled composite structures. PA 12-B_2O_3, PA 12-E-1230, PA 12-E-1400 represent 7.5 wt.% of Boron oxide (B_2O_3), Exolit 1230 and Exolit 1400 filled polymer composite structures, respectively. For composites, test samples were produced with optimum temperature and optimum processing parameters. Table 2.5 demonstrates SLS parameters of Flame Retardant (FR) additive-filled polymer composites.

Table 2.5 : Selective laser sintering process parameters.

Material	Filler Content (%)	Building Chamber Temperature (°C)	Laser Power (W)	Scan Speed (mm/s)	Hatch Distance (mm)	Energy Density (ED) (J/mm^3)
PA 12	0	170	21	2500	0.25	0.336
PA 12-B_2O_3	7.5	173	20	2000	0.25	0.420
PA 12-E-1230	7.5	173	20	2000	0.25	0.420
PA 12-E-1400	7.5	173	20	2000	0.25	0.420

2.3 Characterization Methods

The characterizations in this research have been performed under two different categories: Powder characterization (before SLS processing) and sintered part characterization (after SLS processing).

2.3.1 Powder characterizations

2.3.1.1 Particle size distribution

The particle size distributions of polymer matrix and all used additives were determined by Shimadzu SALD 2300, which measures the particle sizes between 0.02 mm and 2.000 mm.

2.3.1.2 Microstructural analysis

Scanning electron microscopy observations

To examine the powders before SLS processing Hitachi SU3500 T2 SEM (Scanning Electron Microscopy) analyzer was used.

2.3.1.3 Thermal analysis

Differential scanning calorimetry analysis and thermogravimetric analysis

Differential scanning calorimetry (DSC) and thermogravimetric analysis (TGA) measurements were performed using a TA Instruments-SDT 650 thermal analyzer. DSC graphs were utilized to determine the optimal laser processing parameters by determining the sintering window area. Thermal analyses of powders are essential to determine the process conditions. DSC measurements first discovered the “sintering window” area, which is an area between the onset of crystallization and melting

temperatures. Approximately 5 mgs of all the powder samples were heated to 300 °C at a rate of 10 °C/min to observe their melting behavior. Later, the samples were cooled to room temperature at a rate of 5 °C/min to evaluate their crystallization properties.

To assess the homogeneity of the prepared powder mixtures, a thermogravimetric analysis (TGA) test was performed on randomly selected samples from the mixtures. TGA was performed at a rate of 20°C/min up to 700-750 °C.

2.3.2 Sintered sample characterizations

2.3.2.1 Mechanical tests

After SLS processing, the produced samples are called as sintered samples. 3 point bending test and tensile tests were performed using an Instron-3369 with a 50 kN universal testing machine at a 2 mm/min test speed. Quasi-static tensile tests on materials were performed on ISO 527-2 [51] type 1B samples (gage length: 50 mm, width at the narrow portion: 10 mm, distance between the grips: 115 mm, thickness: 4 mm). Flexural test and notched charpy impact tests were done according to ISO 178 [52], ISO 179-1 [53], respectively, with the length of 80 mm, the width of 10, and the thickness of 4 mm dimensioned test samples.

For the Charpy impact test, a Devotrans CD-1 impact test equipment was employed. Dynamic mechanical analysis (DMA) [54] was also carried out in cantilever mode with a Perkin Elmer – DMA 8000 in the temperature range of -100 °C–150 °C, with a scan rate of 1 °C/min and a frequency of 1 Hz.

2.3.2.2 Density measurements

To sintered samples, density measurements were done by a density kit by Precisa XB 220A analytical balance to observe the density alteration of sintered samples with different reinforcement addition.

2.3.2.3 Microstructural analysis

Scanning electron microscopy observations

To examine the sintered samples after SLS production and observe the fracture surcafes of the samples, SU3500 T2 SEM (Scanning Electron Microscopy) analyzer was used.

2.3.2.4 Electrical conductivity test (4-point-probe method)

To examine the metal additive effect on conductivity effect on PA 12 polymer composite structure four-point probe measurements were performed by using a Keithley 2612B Dual – Channel System SourceMeter (SMU).

2.3.2.5 Flame retardancy tests

To investigate the flammability properties of FR filler added polymer composite structures, UL-94 [55] and LOI [56] tests were also performed at related sintered test samples.

3. RESULTS AND DISCUSSION

3.1 Properties of HGM Filled PA 12 Composites

3.1.1 Powder characterizations

3.1.1.1 Particle size distribution

The volumetric particle size distributions of PA 12 and HGM powders are given in Figure 3.1. PA 12 exhibits an average particle diameter of 60 µm, ranging from 20 µm to 250 µm. Moreover, average particle size is determined as 23.5 µm for HGM, also ranging from 3.25 µm to 60 µm.

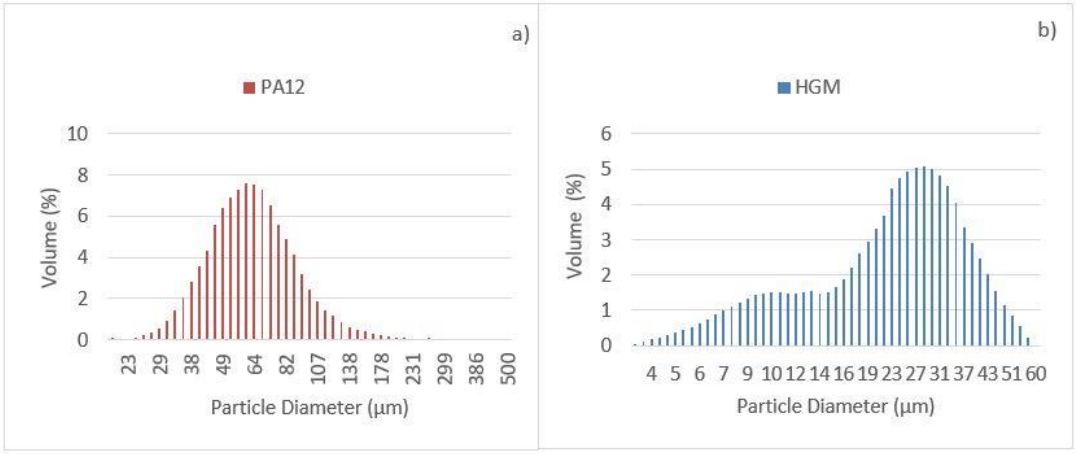

Figure 3.1 : Volumetric particle distribution of a) PA 2200 (EOS), b) iM16K (3M) powders.

3.1.1.2 SEM observations of powders

SEM micrographs of PA 12, HGM and their mixture are given in Figure 3.2. PA 12 particles occur like a potato-like shape with a rough surface, and unlike the PA 12, HGM particles show a perfectly spherical surface.

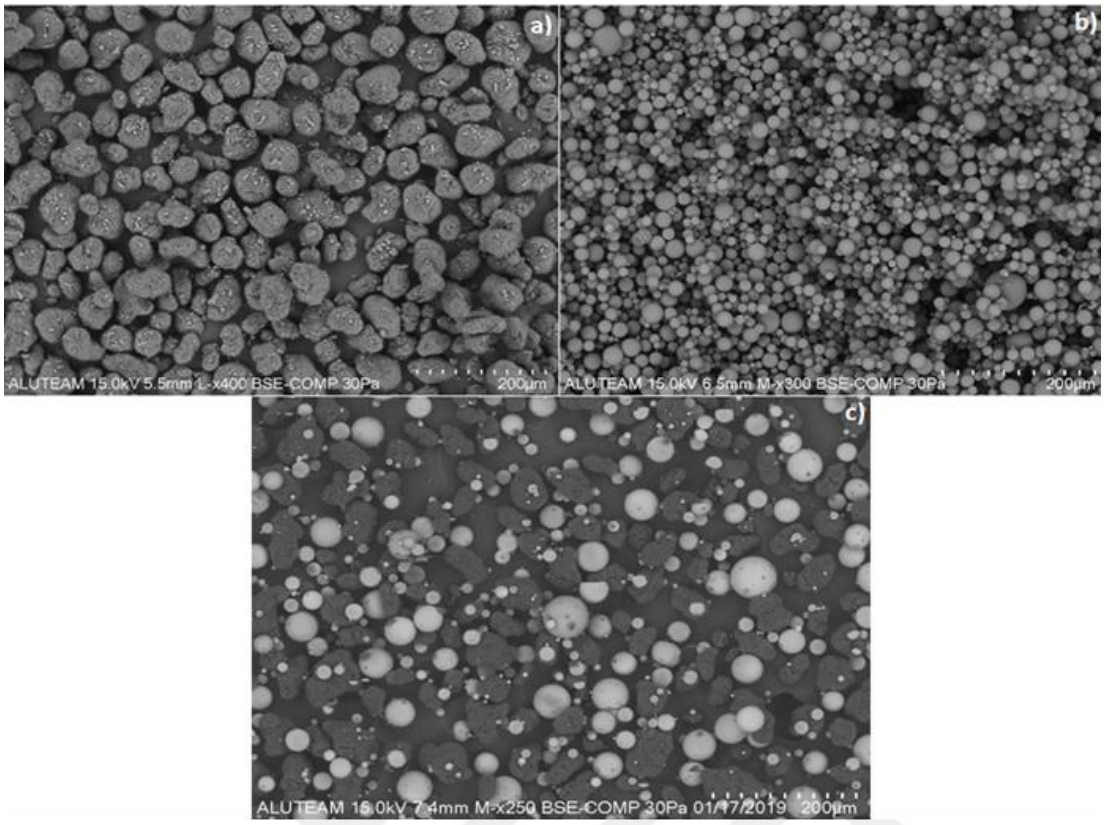

Figure 3.2 : SEM images of powders of a) PA 2200 (EOS), b) iM16K (3M), c) 20% iM16K added PA 2200.

3.1.1.3 Thermal analysis

Differential scanning calorimetry (DSC) analysis and Thermogravimetric analysis (TGA)

Table 3.1 demonstrates the melting (T_m) and the crystallization (T_c) temperatures, and the melting (T_m onset) and the crystallization (T_c onset) onset points for neat PA 12 and all different amounts HGM filled PA 12 mixtures.

Table 3.1 : DSC results: Melting and crystallization temperatures evaluation.

Material	Filler Content (%)	T_m (ºC)	T_m Onset (ºC)	T_c (ºC)	T_c Onset (ºC)	ΔT
PA 12	0	187.59	177.09	139.56	144.53	32.56
PA 12-10HGM	10	187.75	178.20	139.70	144.73	33.47
PA 12-15HGM	15	188.52	179.60	140.42	146.06	33.54
PA 12-20HGM	20	189.00	181.82	145.21	149.02	32.80

Thermogravimetric analysis (TGA) has been conducted for PA 12-10HGM, PA 12-15HGM, PA 12-20HGM. TGA tests were carried out at 20 °C/min up to 700 °C. The

TGA analysis test results given in Figure 3.3 show the obtained residue percentages at 700 °C.

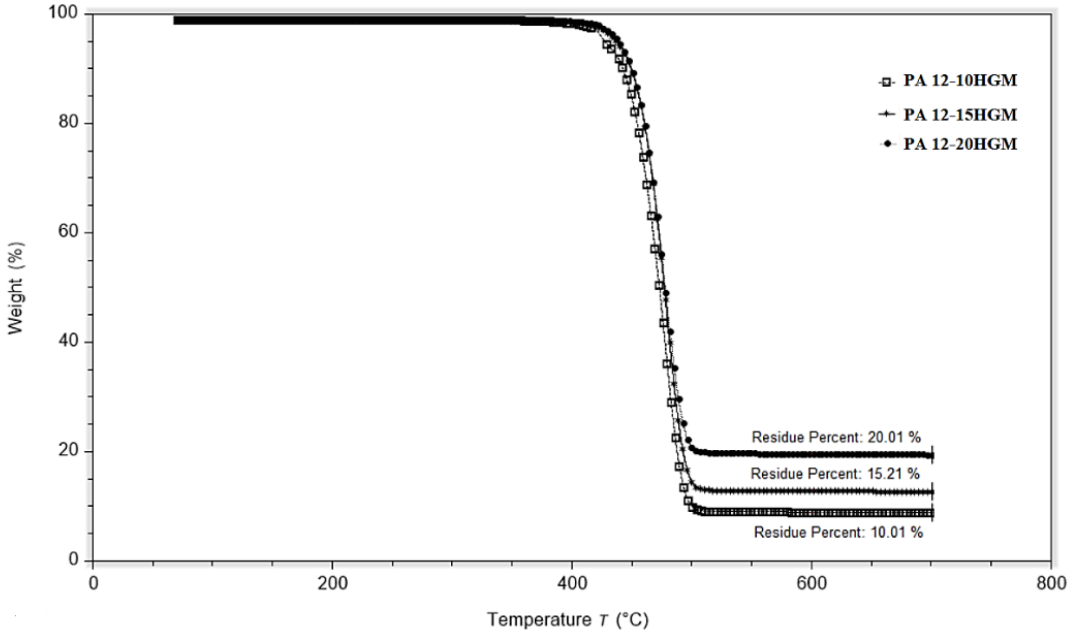

Figure 3.3 : TGA results of PA 12-10HGM, PA 12-15HGM, PA 12-20HGM.

3.1.2 Sintered part characterizations

3.1.2.1 Mechanical test results and density measurements

The mechanical properties of the sintered specimens are investigated by tensile, 3 point bending and notched-charpy impact tests. Results of the tensile, 3 point bending and notched-charpy impact tests are given in Figure 3.4, Figure 3.5 and Figure 3.6, respectively. The average maximum tensile stress of unfilled PA 12 samples was obtained as 48.07 Mpa according to tensile test results. The values of HGM filled PA 12 sintered specimens were changed slightly, and the average maximum tensile test result is around 40 MPa. The tensile modulus and maximum elongation at break value of unfilled PA 12 were 1.66 GPa and 28.99%, respectively. Although there is a small decrease in 15% of HGM added PA 12, E-modulus increases by the addition of the increasing amount of HGM and reaches to 2.75 GPa at 20% of HGM addition. With the addition of HGM, the maximum tensile strain at break values decreases as expected.

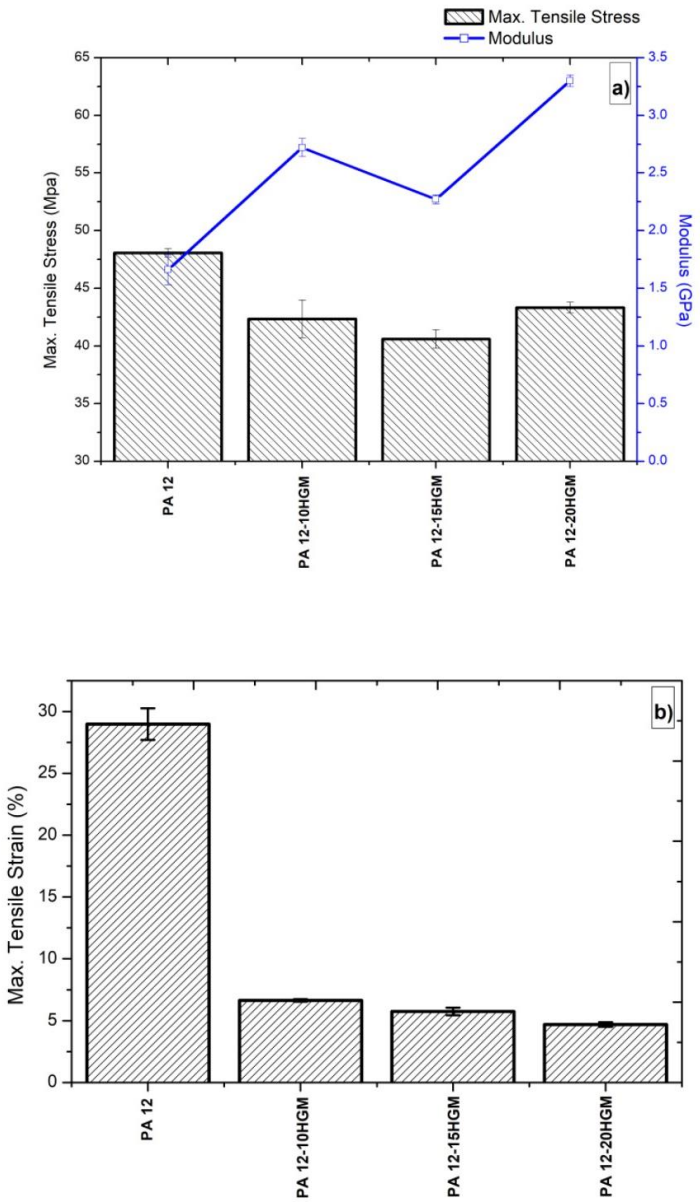

Figure 3.4 : Tensile test results a) Maximum tensile stress, b) Maximum tensile strain.

Figure 3.5 shows 3 point bending flexural test results of unfilled PA 12 and filled ones. 3 point bending test results of neat PA 12 is 1.68 GPa of E-Modulus, 67.58 MPa of maximum flexural stress, and 7.70% of maximum flexural strain. By the addition of the increasing amount of HGM, E-Modulus is reached to higher values when compared to unfilled PA 12. As well as there is a small decrease in 15% of HGM added PA 12, maximum flexural stresses of HGM filled PA 12 composite structures are

changing slightly as 64.26 MPa, 57.04 MPa, 62.33 MPa for PA 12-10HGM, PA 12-15HGM, PA 12-20HGM, respectively.

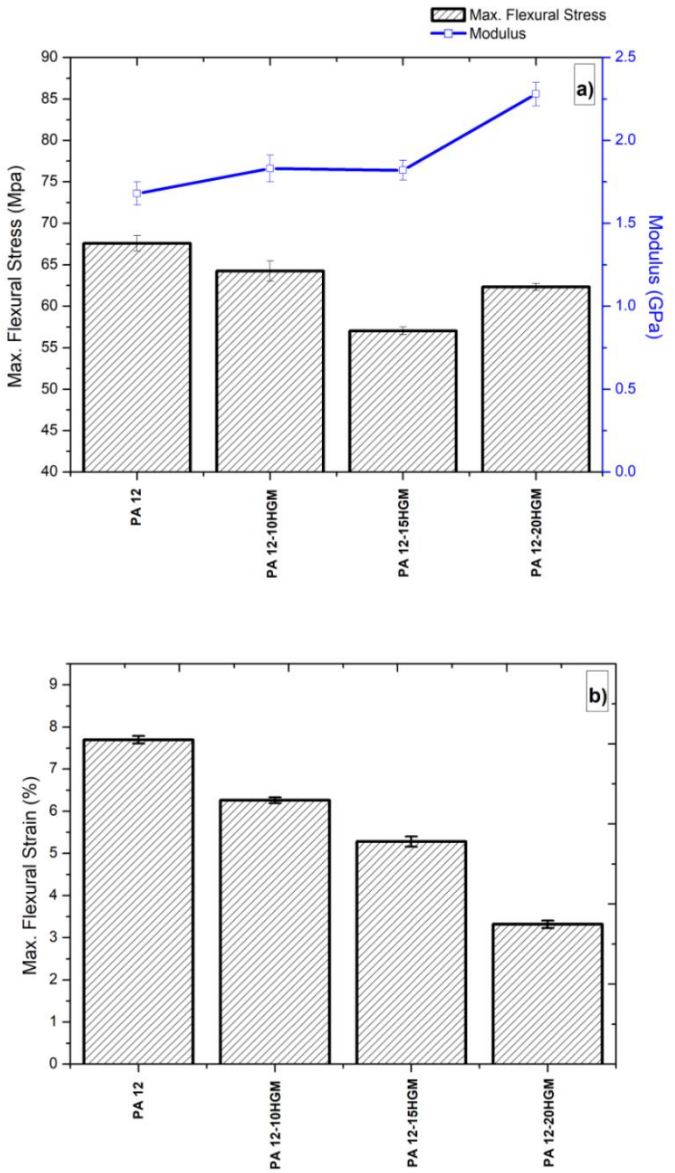

Figure 3.5 : Flexural test results a) Maximum flexural stress, b) Maximum flexural strain.

Figure 3.6 shows notched charpy impact test results of PA 12, and different amounts of HGM filled polymer composite structures. It can be inferred from the test results that the notched charpy impact strength slightly changes until 20% of HGM filler. At 20% of HGM, it comes to 4.70 kJ/m^2.

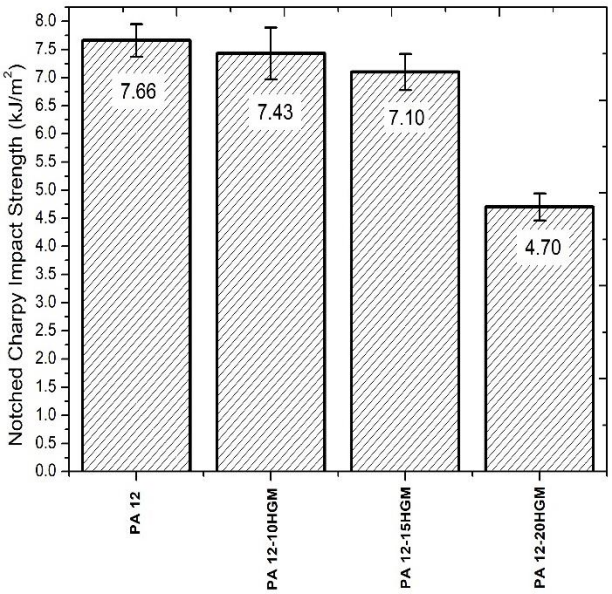

Figure 3.6 : Notched-Charpy impact test results.

The first and the most important purpose of this research is to obtain lighter weight without sacrificing much of the stability and properties of the material. Density measurement results of various amounts of HGM filled PA 12 and neat PA 12 are shown in Figure 3.7. Density values are 1.01 g/cm^3, 0.90 g/cm^3, 0.85 g/cm^3, 0.80 g/cm^3 for neat PA12, PA 12-10HGM, PA 12-15HGM, PA 12-20HGM, respectively. These values correspond to 10.96%, 17.78%, and 20.79% density reduction for 10%, 15% to 20% HGM added structures.

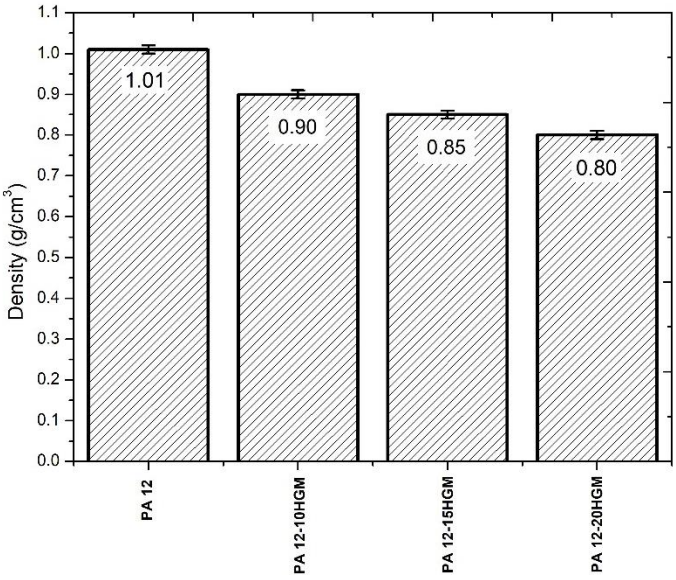

Figure 3.7 : Density measurement of sintered samples.

3.1.2.2 SEM observations of sintered parts

Figure 3.8 shows SEM observations of the cross-sectional areas of HGM filled PA 12 sintered samples after performed mechanical tests.

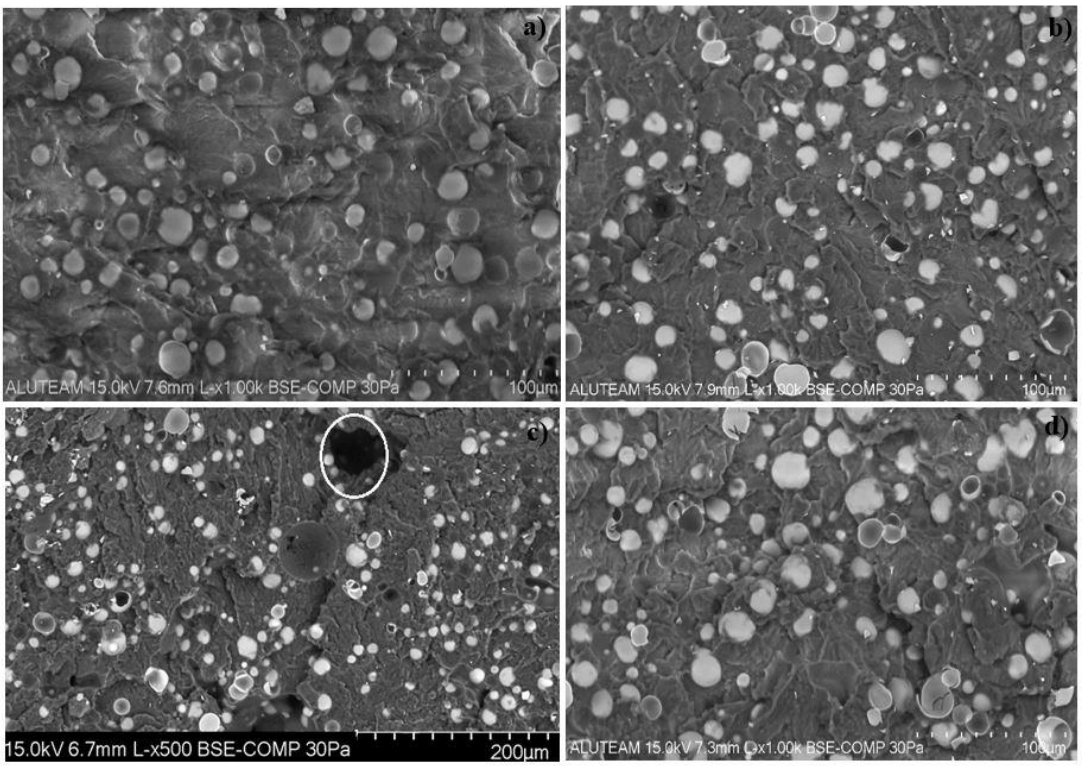

Figure 3.8 : SEM images of sintered composite structures a) PA 12-10HGM-L-x1.00k, b) PA 12-15HGM- L-x1.00k, c) PA 12-15HGM-L-x500, d) PA 12 20HGM – L-x1.00k.

3.2 Properties of different types of HGM Filled PA 12 Composites

3.2.1 Powder characterizations

3.2.1.1 Particle size distribution

The volumetric particle size distributions of PA 12 and all different additives are given in Figure 3.9. The average particle sizes are 60 µm, 55 µm, 45 µm, 23.5 µm, 61.5 µm, 30.5 µm for PA 12, EHGMS-60S, HGB-M60, iM16k HGM, MWS-2575, EHGMS-60, respectively. Consequently, mixtures of PA 12 and different types of HGMs in any ratio will be between two distributions.

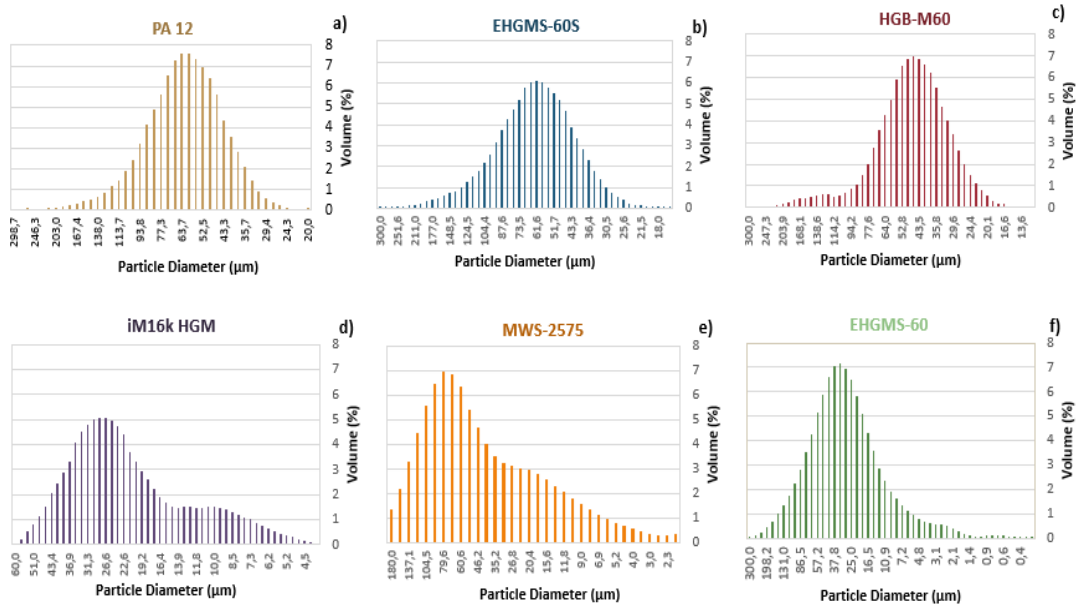

Figure 3.9 : Volumetric particle distribution of a) PA 12, b) EHGMS-60S, c) HGB-M60, d) iM16k HGM, e) MWS-2575, f) EHGMS-60 powders.

3.2.1.2 SEM observations of powders

Before laser sintering processing, polymeric powder and all types of additives were observed under SEM. Figure 3.10 shows SEM images of PA 12 polymer, hollow glass microsphere, and mineral-hollow glass microsphere additives.

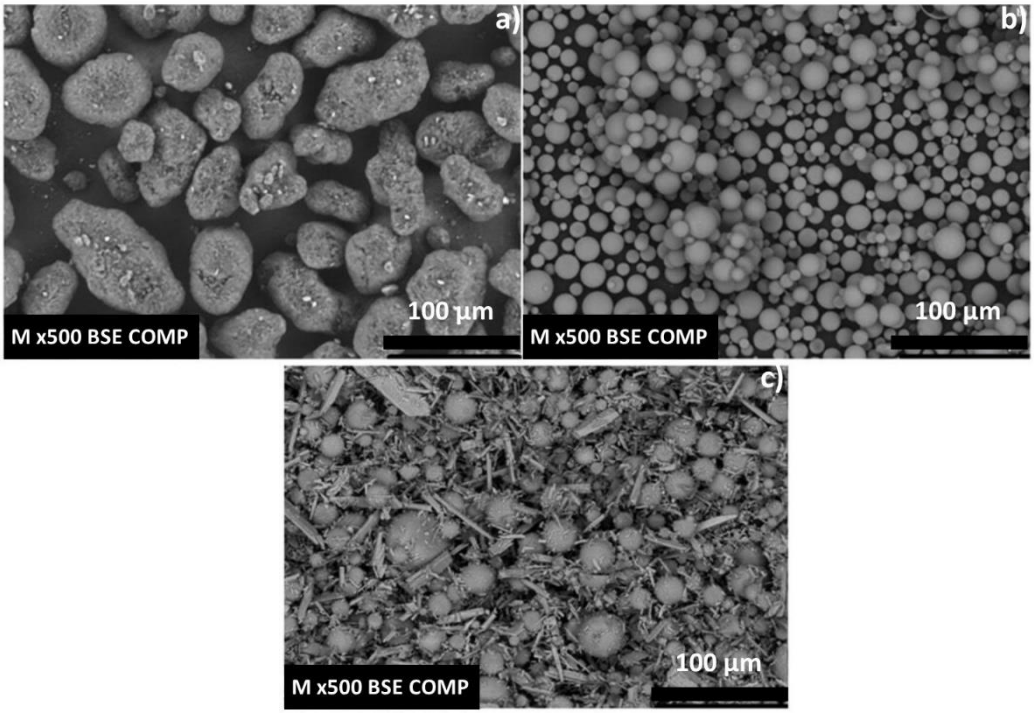

Figure 3.10 : SEM images of the polymer matrix and some of the additives (a)PA 2200 (EOS GmbH), b) iM16k HGM (3MTM), c) MWS 2575 (ELMINAS®))

3.2.1.3 Thermal analysis

Differential scanning calorimetry (DSC) analysis and Thermogravimetric analysis (TGA)

Table 3.2 indicates the melting (T_m) and the crystallization (T_c) temperatures, and the melting (T_m onset) and the crystallization (T_c onset) onset points for unfilled PA 12 and all various types of hollow featured additive filled PA 12 mixtures. According to Table 3.2, ΔT represents the difference between T_m and T_c onset points, which is slightly changing around 32.06-32.80 for the same amount and different types of filler-added polymer composite mixtures.

Also, the crystallinity percentages of unfilled and filled PA 12 structures were detected by dividing the enthalpy obtained from the DSC thermograms by 209.3 J/g [57, 58], which is the known literature value for completely crystalline PA 12 polymeric material. The degree of crystallinity can be calculated by the below formula [57]:

$$\%\ Crystallinity = (\Delta H_{measured}/\Delta H_{known})\ x\ 100\% \quad (3.1)$$

Reinforcing the polymer with particles caused an increase in the percentage of crystallization. The use of hollow featured additives enhanced the degree of crystallization. The number of nuclei may increase which resulting in higher crystallization rates.

Table 3.2 : DSC results: Melting and crystallization temperatures evaluation.

Material	Filler Content (%)	T_m (ºC)	T_m Onset (ºC)	T_c (ºC)	T_c Onset (ºC)	ΔT	Cryst. (%)
PA 12	0	187.59	177.09	139.56	144.53	32.56	28.65
PA 12-20HGS60S	20	187.87	177.44	140.80	144.84	32.60	28.88
PA 12-20HGB	20	187.10	178.84	141.38	146.75	32.09	29.32
PA 12-20HGM	20	189.00	181.82	145.21	149.02	32.80	30.04
PA 12-20MWS	20	189.70	182.78	146.82	150.01	32.77	32.37
PA 12-20HGS60	20	189.87	183.57	146.88	151.51	32.06	33.07

However, Thermogravimetric analysis (TGA) test was performed to demonstrate the homogeneity of all mixtures. TGA has been conducted by TA Instruments SDT 650 thermal analyzer to PA 12-20HGS60S, PA 12-20HGB, PA 12-20HGM, PA 12-20MWS, PA 12-20HGS60, composite mixtures. TGA tests were performed at 20 °C/min up to 700 °C.

3.2.2 Sintered part characterizations

3.2.2.1 Mechanical test results and density measurements

The mechanical properties of the sintered samples are shown in Figures 3.11, 3.12, and 3.13. The tensile properties of unfilled PA 12 are 48.07 MPa of the maximum tensile stress, 1.66 GPa of E-modulus, and 28.99 % of maximum elongation at break value (Figure 3.11). According to tensile tests of manufactured polymer composites, the ultimate tensile stress value changes between 32 MPa-42.5 MPa; E-modulus differs from 2.35 GPa to 2.75 GPa. PA 12-20HGS60S composites have the lowest ultimate tensile and modulus results when compared to other produced composite structures.

Figure 3.12 demonstrates the flexural test results of unfilled PA 12 and various hollow additive-filled polymer composite structures. Three-point bending flexural test results of unfilled PA 12 are 67.58 MPa of maximum flexural stress, 1.68 GPa of E-modulus, and 7.70 % of maximum flexural strain. For flexural test results, it can be said that maximum flexural stress values are between 56 MPa-60 MPa, and flexural modulus changes between 1.65 MPa to 2.30 MPa. When all produced composites were compared, PA 12-20HGS60 and PA 12-20HGM composites give higher tensile and flexural stress results and E-modulus values.

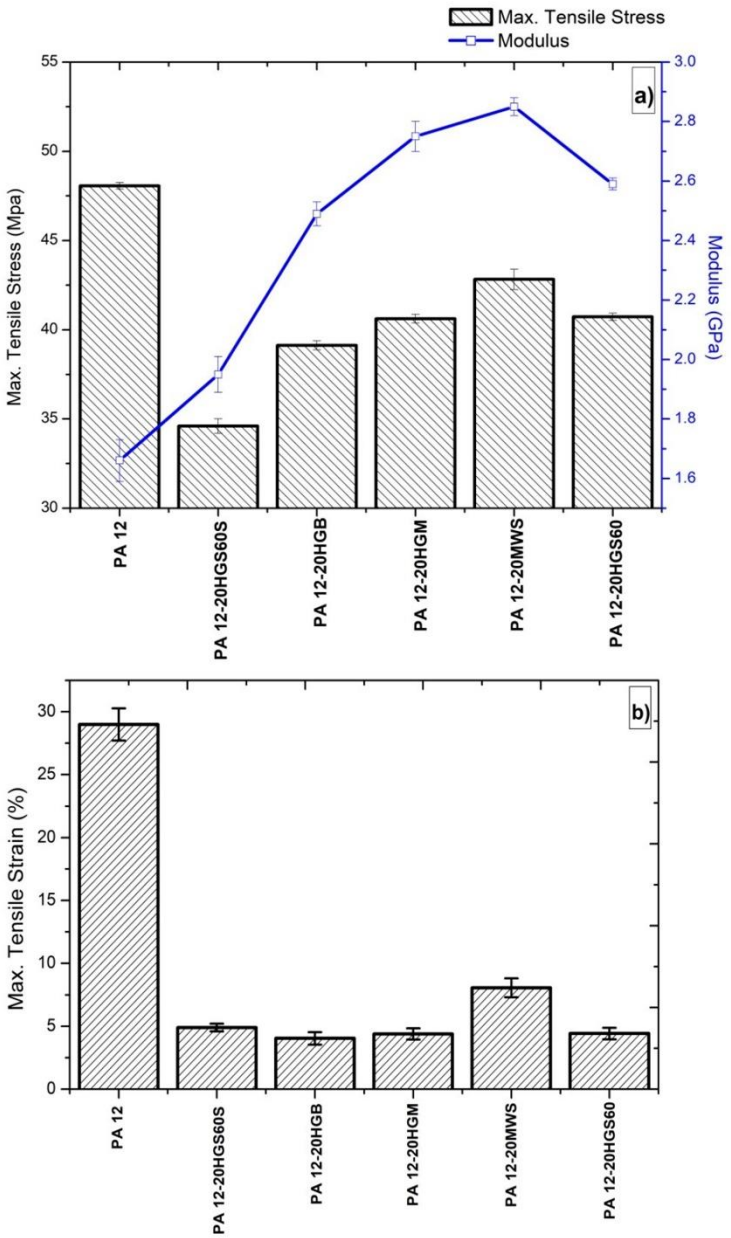

Figure 3.11 : Tensile test results a) Maximum tensile stress, b) Maximum tensile strain.

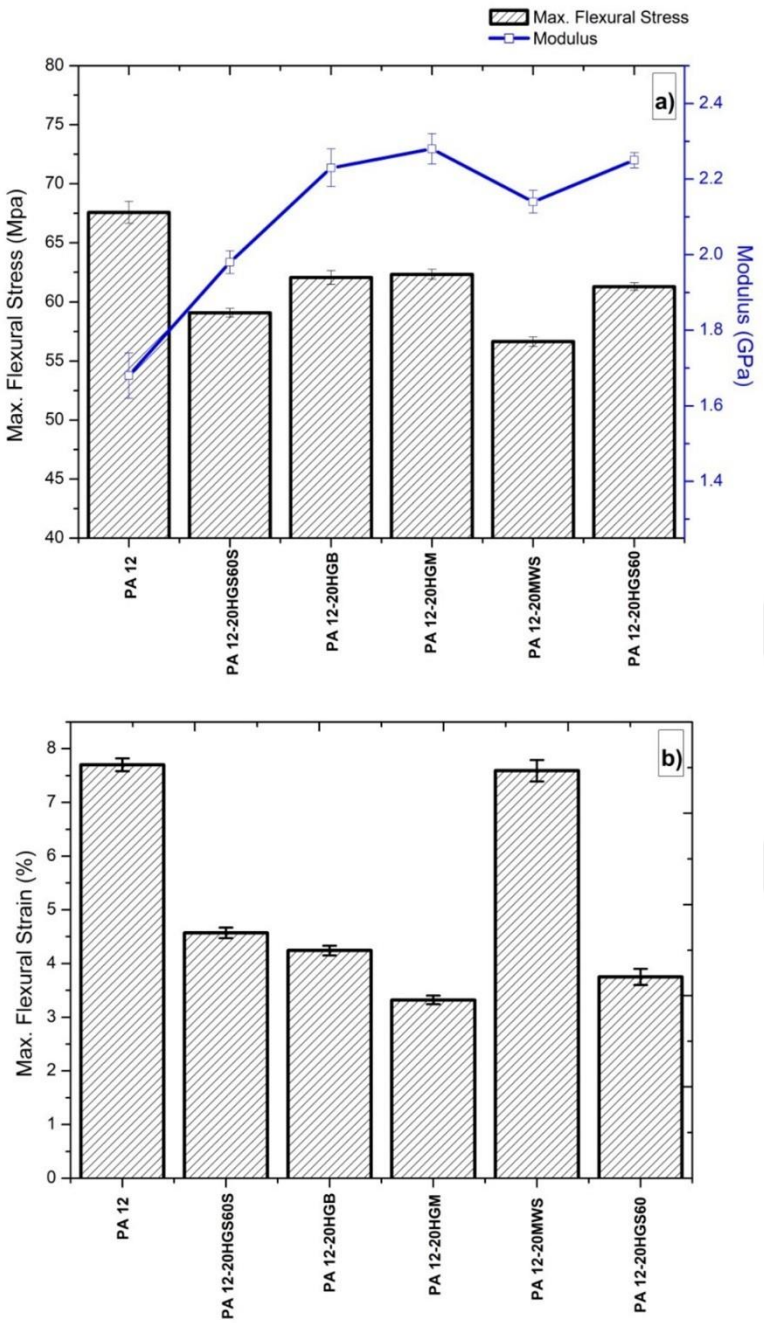

Figure 3.12 : Flexural test results a) Maximum flexural stress, b) Maximum flexural strain.

Figure 3.13 shows notched type Charpy impact test results of unfilled PA 12 and different types of 20% filler added polymer composites. According to the performed tests, it can be inferred that the notched Charpy impact strength of PA 12-20MWS (7.48 kJ/m^2) composites are the closest to the test result of PA 12 itself (7.66 kJ/m^2). For PA 12-20HGS60S and PA 12-20HGS60, the values are 6.77 kJ/m^2 and 6.03 kJ/m^2, respectively. However, PA12-20HGB and PA 12-20HGM composites exhibit lower impact test results, which are around 5.20-5.25 kJ/m^2, than other types. The impact

strength values showed a different behavior with the values obtained from the tensile and bending tests. The change of loading type during the impact test and the prominence of the energy value that the material will absorb during the test have caused the material behavior to change. The use of oxide-based particles with high strength and brittleness has led to a decrease in absorbed energy. On the other hand, using MWS-2575 additive, which contains spherical and rod-shaped particles, increased the absorbed energy and increased the impact strength value.

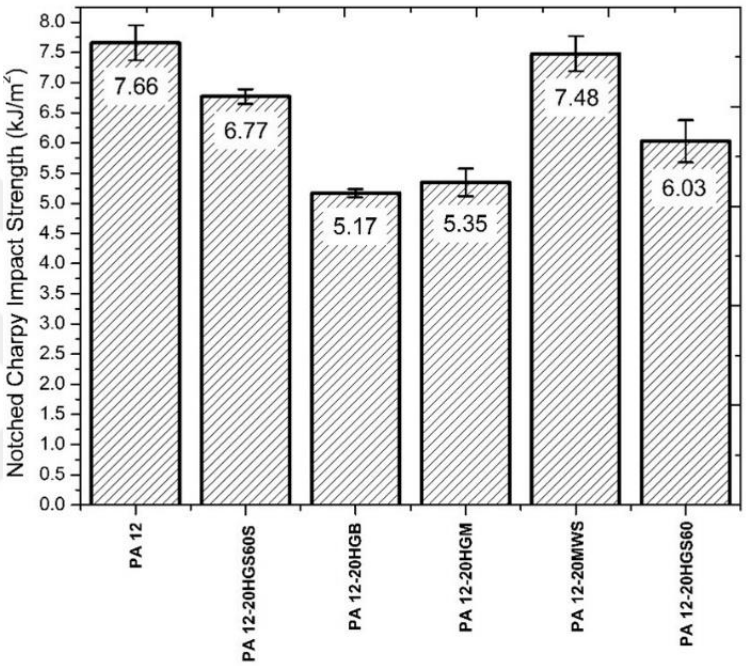

Figure 3.13 : Notched Charpy impact test results.

Figure 3.14 gives the density test measurement comparison of unfilled polymer and filled polymer composite structures. The highest density reduction was obtained from PA 12-20HGM composite structure, which is 20% reduction compared to unfilled PA 12. Density measurement results of PA 12-20HGS60S and PA 12-20HGS60 polymer composites were 0.86 g/cm^3. PA 12-20HGB follows it with a result of 0.88 g/cm^3. However, PA 12-20MWS has 1.03 g/cm^3 density value. Although hollow glass microsphere is added to the polymer matrix, there is no decrease in density because the related additive also has mineral addition as a declaration from the corresponding additive TDS. Since both the hollow glass microsphere and the mineral addition are together, which does not allow a density drop in the composite structure.

The main purpose of the study is as well as to obtain lightweighted PA 12 composite structures and examine the physical and mechanical property changes that will occur

in PA 12 in the composite materials to be produced. A significant reduction has been achieved in the density of sintered polymer composites produced by reinforcing PA 12. While 14.15% density reduction was achieved for PA 12-20HGS60S and PA12-20HGS60 composites compared to PA 12, this rate reached 20.8% for PA12-20HGM composite structure.

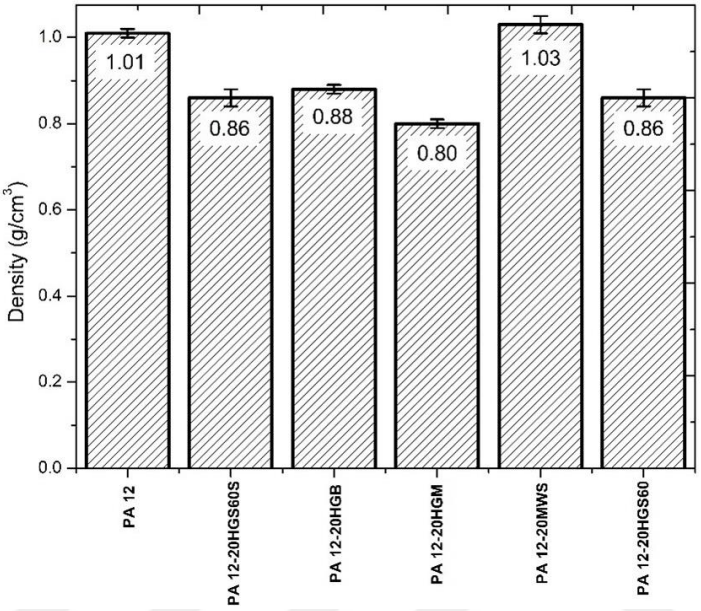

Figure 3.14 : Density measurements.

3.2.2.2 SEM observations of sintered parts

After performed mechanical tests, fracture surface microscopy (SEM) analyses of unfilled and filled PA 12 sintered samples were also done (in Figure 3.15 and Figure 3.16).

In Figure 3.15, images were taken from the fracture surfaces of the samples after the tensile test. Among the reinforced samples, the highest tensile strength value was obtained in the sample coded PA 12-20MWS. The lowest tensile strength value was obtained in the sample coded PA 12-20HGS60S. When the fracture surfaces of the samples coded PA 12-20HGS60S, PA 12-20HGM, and PA 12-20HGS60 were examined, voids in the matrix structure were evident. These voids in the matrix structure hindered the load transfer from the matrix to the reinforcements.

The integrity of the PA 12 matrix structure during the tensile test ensured that the load generated during the test was transferred to the reinforcement element by the matrix for PA 12-20HGB and PA 12-20MWS coded samples. For this reason, high stresses

have occurred on the reinforcement element, and as seen in both fracture surface images, the reinforcement elements have been separated from the matrix from place to place. This situation was more evident in the sample coded PA 12-20HGB. After the tensile test, a very hollow structure emerged due to filler pull-outs on the fracture surface of this sample. This was possibly realized because of the poor interfacial connection between filler and matrix. In the PA 12-MWS coded sample, on the other hand, the matrix-reinforcement element interfacial connection was formed more strongly with much fewer filler pull-outs and voids; thus, the highest tensile strength value was obtained.

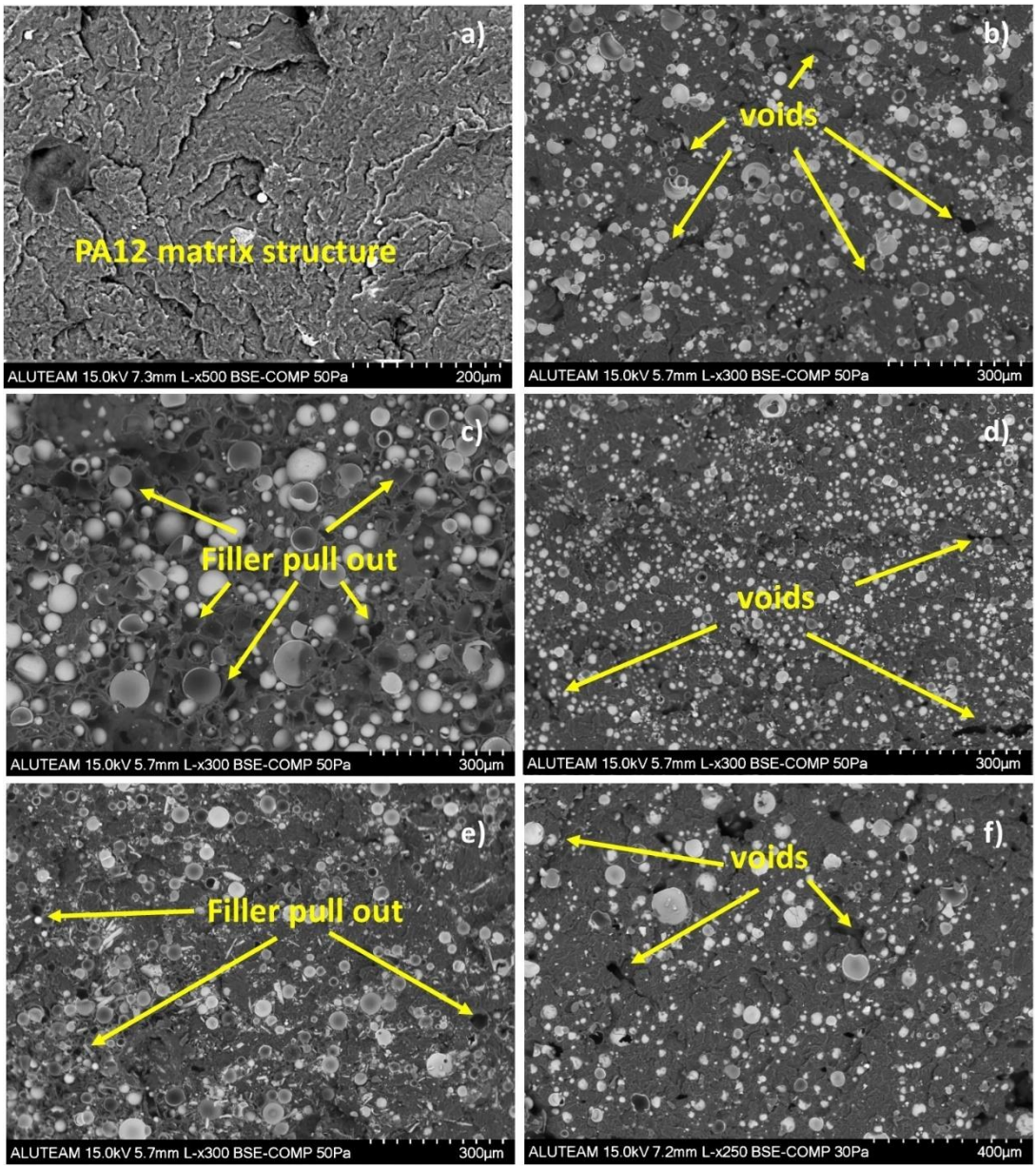

Figure 3.15 : SEM observations of fracture surfaces after tensile test a) unfilled PA 12, b) PA12-20HGS60S, c) PA12-20HGB, d) PA12-20HGM, e) PA12-20MWS, f) PA12-20HGS60.

SEM images of fracture surfaces resulting from the impact test were given in Figure 3.16. It was observed that severe matrix fracture took place at the samples PA 12-20HGB and PA 12-20HGM, where the impact energy was the lowest. It was also evident that matrix fracture that occurred in these samples had a negative effect on the impact energy of the material. The samples that provide the better impact test performance among composite materials are PA 12-20HGS60S and PA 12-20HGS60 coded samples. When the fracture surfaces of these samples were examined, only a few voids could be seen in the composite structures. Particularly in the sample with the code PA 12-20MWS, it was determined that the reinforcement elements also contributed to the impact energy absorption owing to the usage of rod-shaped and spherical filler mixture. This allowed the sample with the code PA 12-20MWS to show the best performance during the impact test among composite materials.

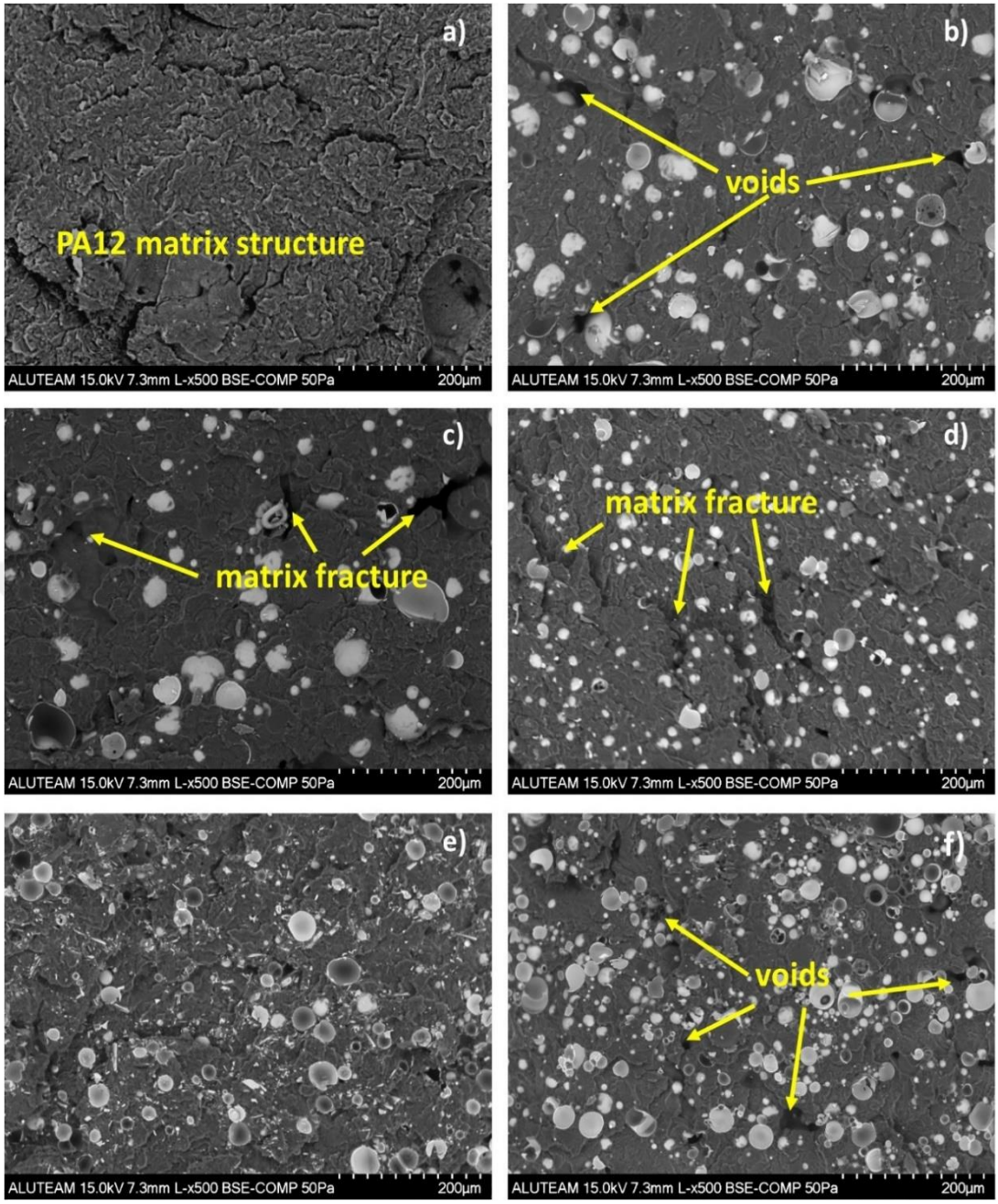

Figure 3.16 : SEM observations of fracture surfaces after impact test a) unfilled PA 12, b) PA12-20HGS60S, c) PA12-20HGB, d) PA12-20HGM, e) PA12-20MWS, f) PA12-20HGS60.

3.3 Properties of Different Types of Cu Filled PA 12 Composites

3.3.1 Powder characterizations

3.3.1.1 Particle size distribution

Figure 3.17 demonstrates the volumetric particle size distributions of PA 12, dendritic, and spherical Cu powder particles. The average particle sizes are 60 µm, 63 µm, and 90 µm for PA 12, dendritic Cu, and spherical Cu.

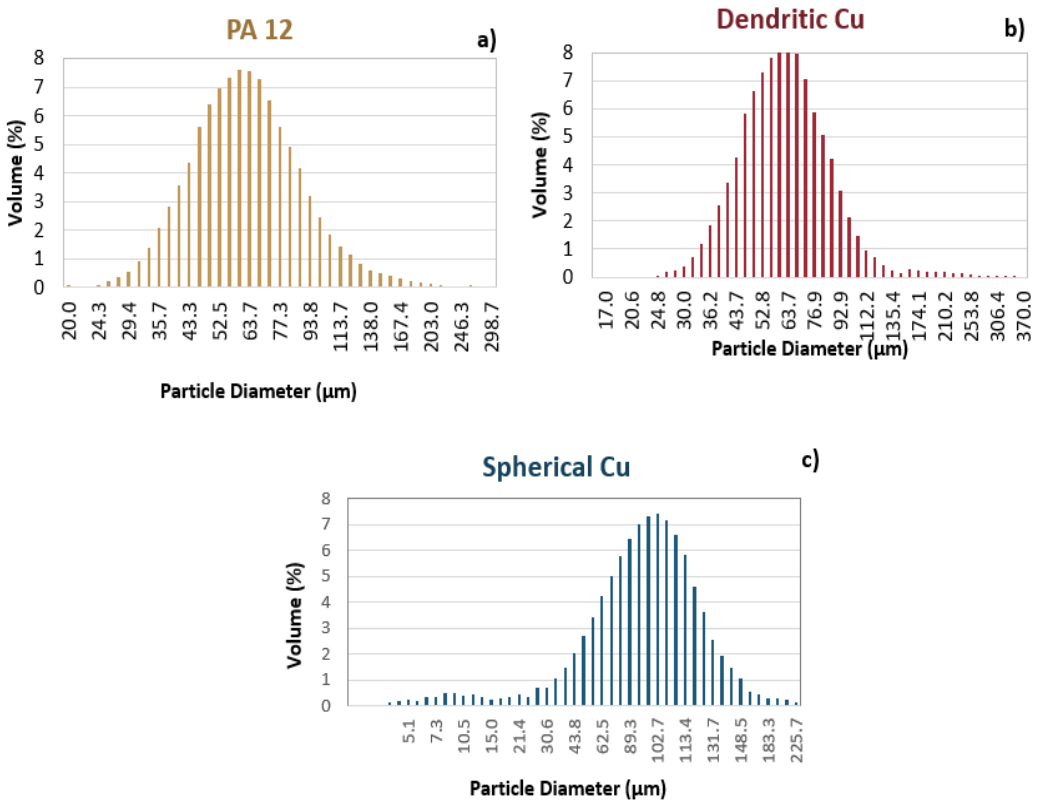

Figure 3.17 : Volumetric particle distribution of a) PA 12, b) Dendritic Cu powder, c) Spherical Cu powder.

3.3.1.2 SEM observations of powders

SEM micrographs for PA 12, spherical, and dendritic Cu and prepared composite powders can be seen in Figure 3.18.

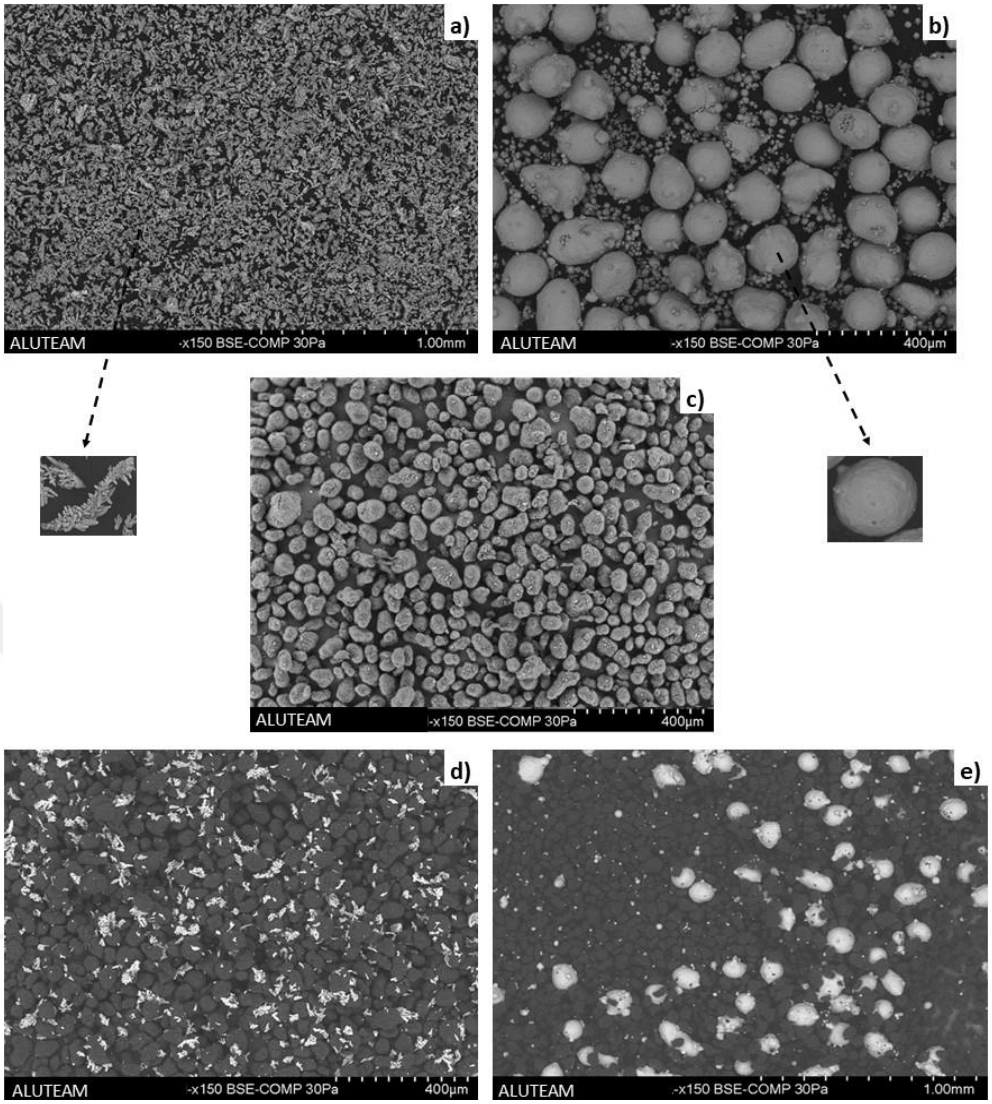

Figure 3.18. SEM Images of a) Dendritic Cu, b) Spherical Cu, c) PA 12 polymer powders, d) PA 12-Dendritic Cu mixture, e) PA 12-Spherical Cu mixture.

3.3.1.3 Thermal Analysis

Differential scanning calorimetry (DSC) analysis and Thermogravimetric analysis (TGA)

Table 3.3 indicates the melting (T_m) and the crystallization (T_c) temperatures, and the melting (T_m onset) and the crystallization (T_c onset) onset points for neat PA 12, dendritic, and spherical Cu-filled PA 12 mixtures. Table 3.3 also shows the temperature difference (ΔT) between the melting and crystallization onset points, which was found to range between 31-32.5 °C.

The addition of Cu fillers to polymer increased both crystallization temperatures. T_c onset temperatures of both Cu-filled compositions were 2.5-3 °C higher than the neat

PA 12. It might be because fillers act as nucleating agents, influencing the crystallization behavior of the structures. As a result, greater ED values and/or higher processing temperatures, or both, may be required [25, 49].

However, the crystallinity percentage was determined by dividing the melting enthalpy obtained from the DSC thermograms by 209.3 J/g [57, 58], which is the known literature value for completely crystalline PA 12 polymeric material. The formula below can be used to calculate the degree of crystallinity [58].

$$\% \, Crystallinity = (\Delta H_{measured}/\Delta H_{known}) \, x \, 100\% \qquad (3.1)$$

The use of copper fillers also enhanced the degree of crystallization. The number of nuclei may rise with Cu concentration, resulting in higher crystallization percentages.

Table 3.3 : DSC results: Melting and crystallization temperatures evaluations.

Material	Filler Content (%)	T_m (ºC)	T_m Onset (ºC)	T_c (ºC)	T_c Onset (ºC)	ΔT	Cryst. (%)
PA12	0	187.59	177.09	139.56	144.53	32.56	28.64
PA12-D	15	189.71	178.26	141.55	147.19	31.07	30.74
PA12-S	15	189.29	178.78	141.58	147.35	31.43	31.77

TGA was performed on dendritic and spherical copper filler added mixtures to determine the prepared mixtures' homogeneity. Tests were applied to three samples taken randomly from each mixture. Figure 3.19 shows TGA test results for both mixtures. For both, 15% residue percentage was detected at 750 °C.

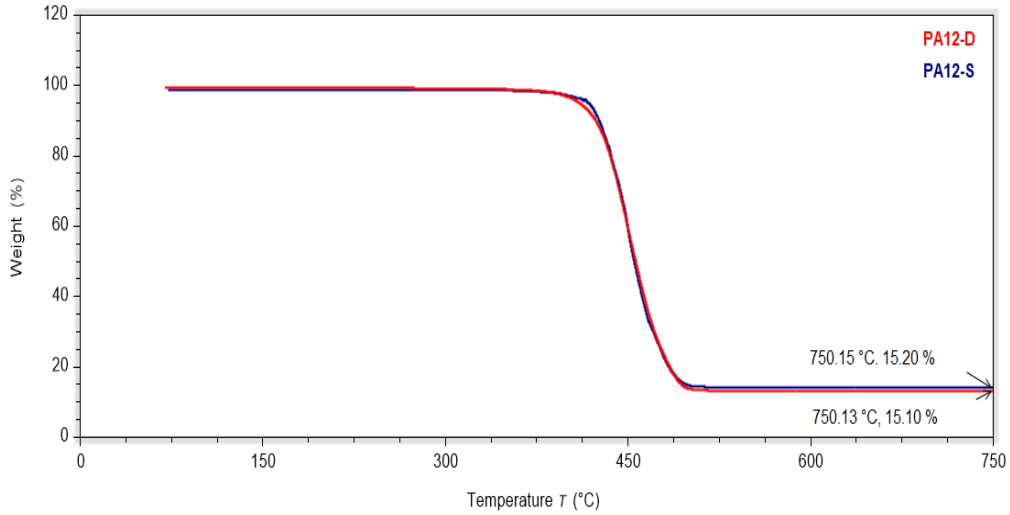

Figure 3.19 : TGA test results of PA12-S, PA12-D.

3.3.2 Sintered part characterizations

3.3.2.1 Mechanical test results

Dynamic Mechanical Analysis (DMA), 3 points bending test, and Charpy impact tests were made to observe the mechanical properties of sintered samples.

With the DMA test, the thermo-mechanical behavior of the sintered samples was examined in terms of storage modulus (E') and loss modulus (E'') as a function of temperature. Transition temperatures were also detected from the tan δ peaks (the ratio of E' to E''). The results at β transition (T_β), 23 ºC, and glass transition (T_g) temperatures are provided in Table 3.4. It was observed that the transition temperature and all modulus values rose with the Cu addition. A reason for this increase could depend on the crystallinity percentage in samples, which was found increasing with Cu fillers, as seen from Table 3.4. main lead in the rise in mechanical values. Although no clear effect between ED and filler types was determined on transition temperatures, spherical filler gave slightly better modulus values.

Table 3.4 : DMA data of PA 12 and Cu-filled PA 12 at T_β, 23ºC and T_g.

Material	ED (J/mm^3)	T_β (^0C)	T_g (^0C)	E' @T_β (GPa)	E' @ 23^0C (GPa)	E' @T_g (GPa)	E'' @T_β (GPa)	E'' @ 23^0C (GPa)	E'' @T_g (GPa)
PA 12	0.34	-71.40	56.50	1.433	1.018	0.561	0.052	0.027	0.052
PA 12-D	0.42	-66.51	60.53	5.669	4.480	2.339	0.197	0.072	0.187
PA 12-D	0.43	-65.41	60.83	5.608	4.473	2.345	0.198	0.078	0.190
PA 12-D	0.44	-70.09	61.08	5.903	4.633	2.388	0.192	0.066	0.190
PA 12-D	0.46	-69.78	60.04	6.215	4.833	2.579	0.210	0.080	0.206
PA 12-D	0.47	-64.44	60.66	5.946	4.737	2.516	0.213	0.074	0.208
PA 12-S	0.42	-67.16	61.44	6.115	4.885	2.466	0.209	0.084	0.213
PA 12-S	0.43	-67.84	61.20	5.829	4.585	2.331	0.199	0.075	0.199
PA 12-S	0.44	-68.16	60.56	6.457	5.097	2.622	0.216	0.079	0.222
PA 12-S	0.46	-67.20	61.20	6.161	4.917	2.529	0.214	0.074	0.218
PA 12-S	0.47	-61.40	61.44	6.415	5.123	2.565	0.225	0.074	0.219

The bending test is one of the most commonly applied mechanical tests on SLS parts. Unfilled one had 67,58 MPa flexural strength and 1680 MPa modulus values. Other results for filled samples are given in Figure 3.20. All flexural test results were higher than unfilled PA 12, which indicates both the reinforcing effect of the filler and the crystallinity increase in PA 12. Spherical-filled samples exhibited higher results than

dendritic-filled ones. However, there was an insignificant change in the ultimate strength values with increasing energy density in both Cu-filled composites. Modulus results for dendritic and spherical filled structures slightly decreased with increasing ED values.

Another mechanical test applied to sintered parts was the Charpy impact test. It was determined that unfilled PA 12 had 7,66 kJ/mm^2 impact strength. Results of the filled samples are given in Figure 3.21. It was seen that all obtained values for the filler samples were lower than neat PA 12. The fillers are discontinuities in the polymer matrix, which results in a decline in impact resistance and causes brittleness.

Moreover, sharp dendrites possibly cause a notch effect in structure, leading to lower impact results. However, there was a significant increase in values with the increasing energy density, especially in dendritic Cu-filled samples. Although dendritic ones reported the lowest impact strength at room temperature, their values rose to those of spherical ones with increasing ED. According to the increasing tendency in ED, it can be said that ED of 0.47 J/mm^3 gave the highest values for both types.

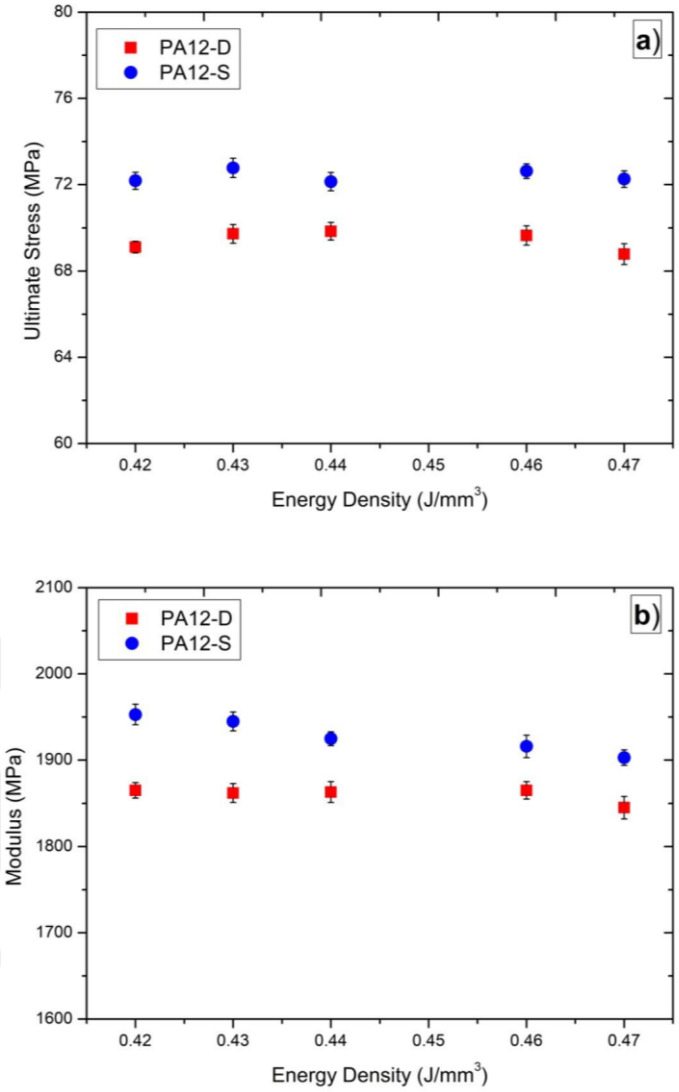

Figure 3.20 : Flexural properties at various ED values a) Ultimate Stress b) Modulus**.**

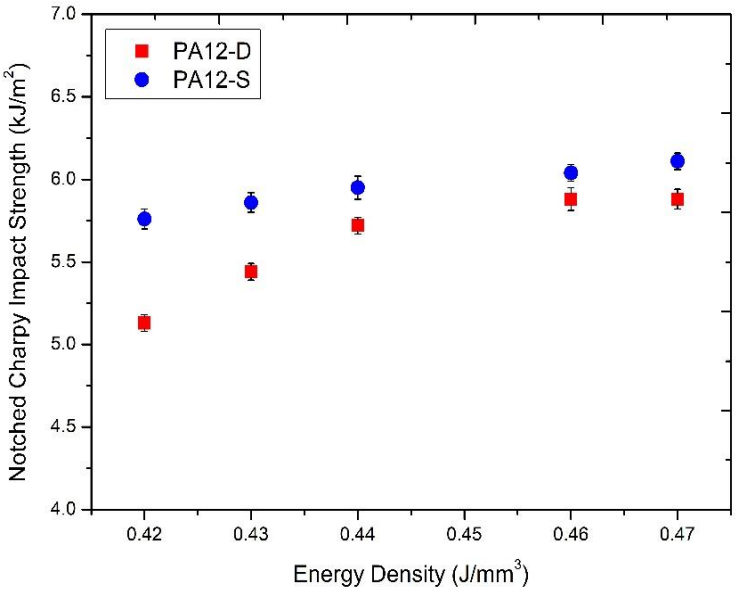

Figure 3.21 : Charpy impact test results.

3.3.2.2 SEM observations of sintered parts

Fracture surfaces after impact tests were observed in SEM, as seen in Figure 3.22. As can be observed in the figure, Cu particles glow in a darker PA 12 matrix. Shapes of both dendritic and spherical particles can obviously be distinguished. No apparent agglomerations or voids were seen in SEM images.

Smaller average particle size and narrower size distribution provide a more uniform mixture. Therefore, dendritic copper-filled composite structures displayed a more homogeneous distribution as in sintered parts. The particle size dispersion of the spherical copper filler is wider.

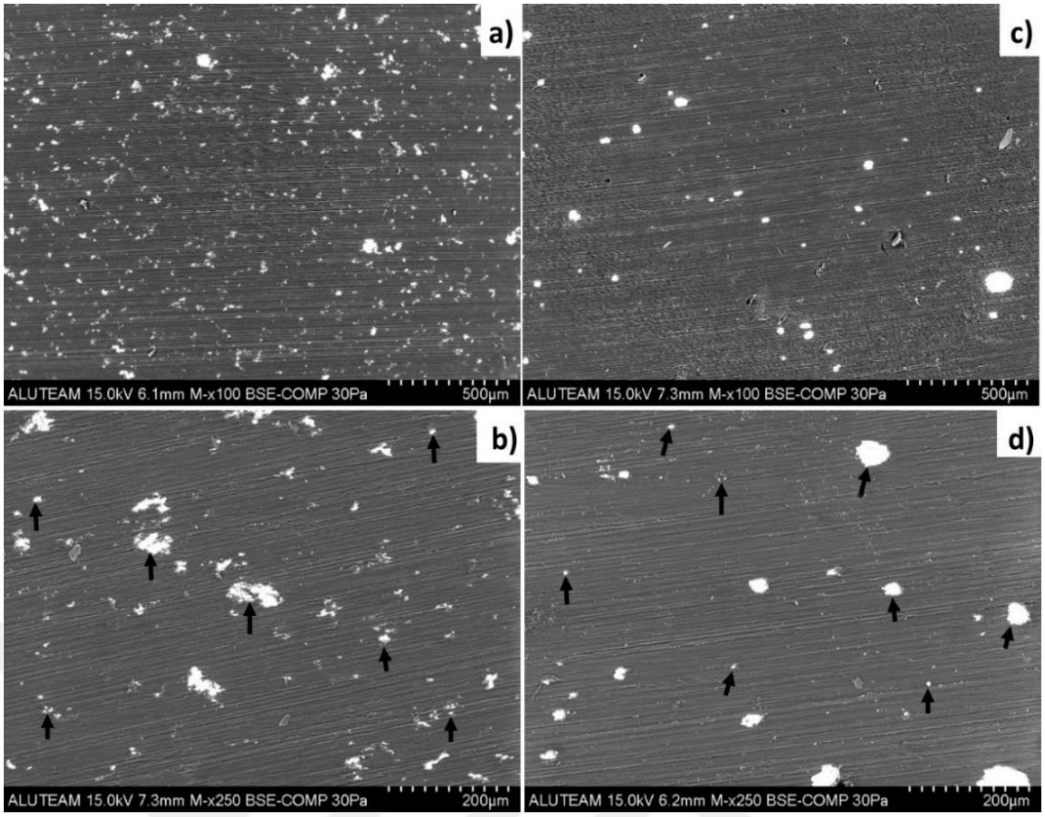

Figure 3.22 : SEM images of a), b) Dendritic Cu-filled sintered samples; c), d) Spherical Cu-filled sintered samples (the black arrows indicate copper reinforcements).

3.3.2.3 Electrical test results (4-probe measuring method)

Electrical conductivity measurements (four-point probe method) were done to unfilled and filled polymer structures. And the sheet resistance of neat PA 12 and Cu-filled composite structures was calculated by the following formula [59]:

$$\rho_s = \frac{V}{I} . \frac{\pi}{ln\ 2} \tag{3.2}$$

Where V is the measured voltage versus applied current as I and ρs is the sheet resistance of materials [60].

Conductivity measurement results of the unfilled and Cu-filled polymers are shown in Figure 3.23. The figure illustrates the electrical conductivity results of dendritic and spherical Cu-filled PA 12 composites at different EDs. The conductivity value of unfilled PA 12 is 7.40x10-11S/cm. The figure illustrates the conductivity measurement results of dendritic and spherical Cu-filled PA 12 composites at different EDs. According to the test results, while it can be said that the electrical conductivity values of the spherical and dendritic Cu-filled samples were higher than the neat polymer.

While conductivity values in spherical Cu-filled samples improved significantly by increasing ED, dendritic Cu-filled samples remained nearly constant as ED increased.

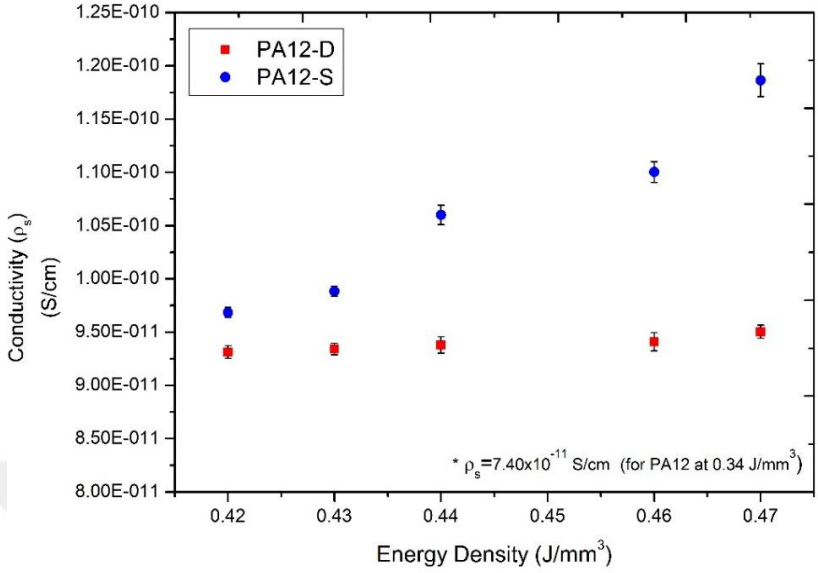

Figure 3.23 : Conductivity values of PA 12 and Cu-filled PA 12 samples.

3.4 Properties of Flame Retardant Additive Filled PA 12 Composites

3.4.1 Powder characterizations

3.4.1.1 Particle size distribution

The volumetric particle size distributions of PA 12 and all different flame retardant (FR) additives are given in Figure 3.24. The average particle sizes are 60 µm, 45 µm, 35 µm, 45 µm for PA 12, B_2O_3, Exolit 1230, Exolit 1400, respectively.

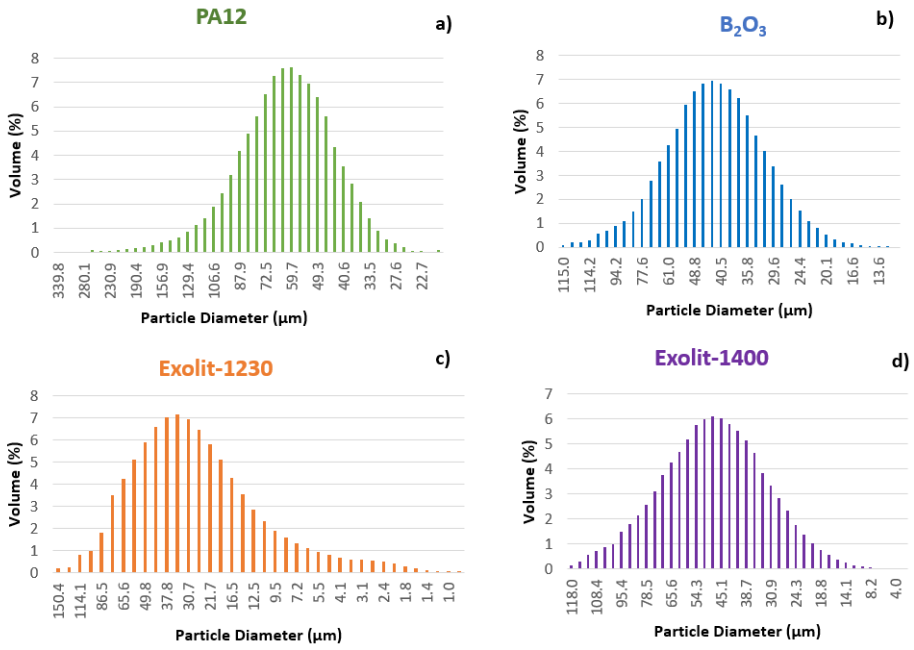

Figure 3.24 : Volumetric particle distribution of a) PA 12, b) B_2O_3, c) Exolit-1230, d) Exolit 1400.

3.4.1.2 SEM observations of powders

SEM micrographs for PA 12, B_2O_3, Exolit 1230, Exolit 1400, be seen in Figure 3.25.

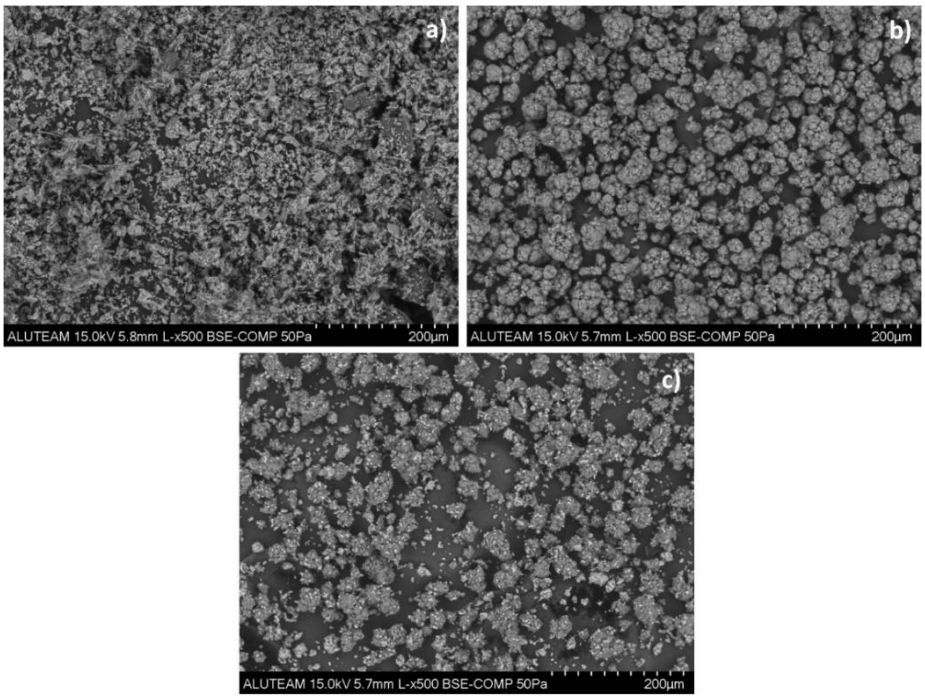

Figure 3.25 : SEM images of filler powders: a) B_2O_3, b) Exolit 1230, c) Exolit 1400.

3.4.1.3 Thermal analysis

Differential scanning calorimetry (DSC) analysis and Thermogravimetric analysis (TGA)

Table 3.5 indicates the melting (T_m) and the crystallization (T_c) temperatures, and the melting (T_m onset) and the crystallization (T_c onset) onset points for neat PA 12, 7.5 wt. % of B_2O_3, Exolit 1230 and Exolit 1400 filled PA 12 mixtures. Table 3.5 also shows the temperature difference (ΔT) between the melting and crystallization onset points, which was found to range between 32.5-36.5 °C.

Table 3.5 : DSC results: Melting and crystallization temperatures evaluations.

Material	Filler Content (%)	T_m (ºC)	T_m Onset (ºC)	T_c (ºC)	T_c Onset (ºC)	ΔT
PA12	0	187.59	177.09	139.56	144.53	32.56
PA 12-B_2O_3	7.5	188.74	181.74	139.67	145.07	36.67
PA12-E 1230	7.5	188.86	180.31	140.45	145.79	34.52
PA12-E 1400	7.5	188.31	181.47	141.95	146.09	33.38

On the other hand, Thermogravimetric analysis (TGA) test was performed to demonstrate the homogeneity of all prepared mixtures. TGA has been conducted by TA Instruments SDT 650 thermal analyzer to PA 12-B_2O_3, PA 12-E-1230, and PA 12-E, composite mixtures. TGA tests were performed at 20 °C/min up to 700 °C.

3.4.2 Sintered part characterizations

3.4.2.1 Mechanical test results and density measurements

Maximum tensile strength, E-modulus and elongation values of composite materials produced with PA 12 are given in Figure 3.26. B_2O_3, with high mechanical strength and hardness, is a ceramic-based additive used to reinforce PA 12. E-1230 and E-1400 are hydrocarbon-based reinforcement materials. A high maximum tensile strength and modulus values were obtained in the composite material obtained by using this reinforcement material. However, the increase in mechanical strength caused embrittlement of the material and a significant decrease in the elongation values. Similar strength and elongation values were obtained in composite materials obtained by using E-1230 and E-1400 materials.

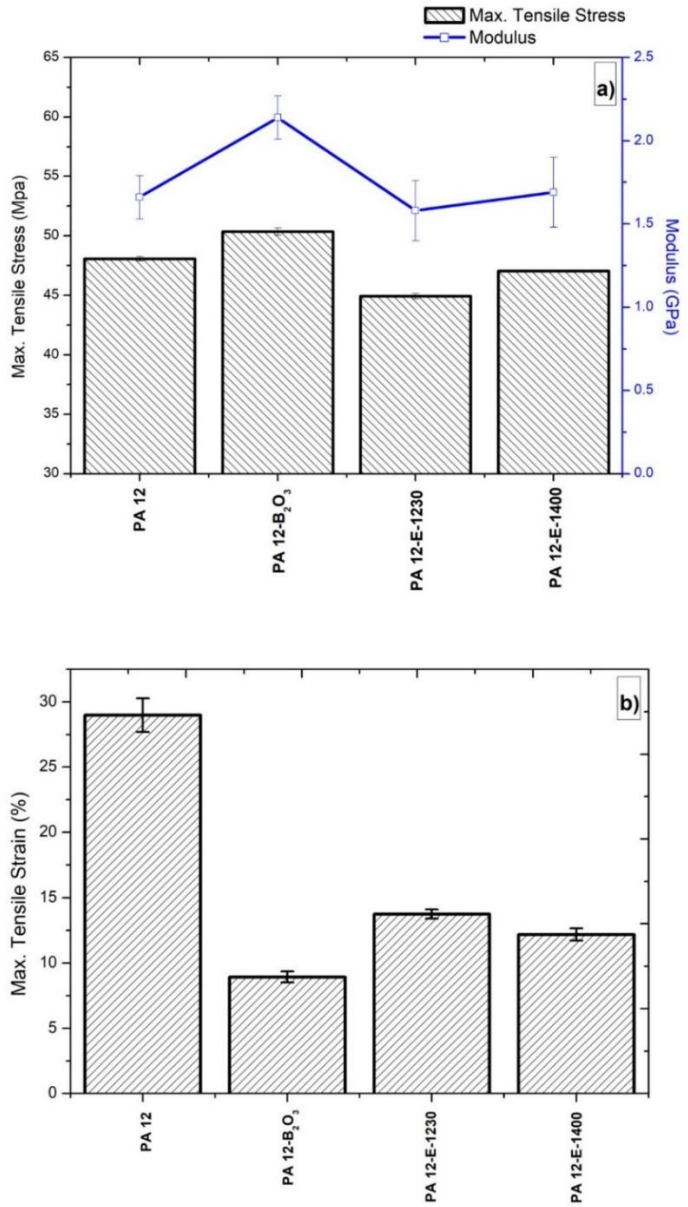

Figure 3.26 : Tensile test results of a) PA 12-B_2O_3, b) PA 12-E-1230, c) PA 12-E-1400 composite structures.

When the data obtained as a result of the bending test were examined (Figure 3.27), similar mechanical behavior was observed with the data obtained as a result of the tensile test. The flexural strength of the material increased significantly with the use of B_2O_3 as a reinforcing element. The reinforcing element with high mechanical strength and hardness increased the flexural strength of the PA 12 matrix. When the modulus values were examined, it was observed that the B_2O_3 structure provided the highest modulus value. However, with the use of B_2O_3, the brittleness of the material increased, and the lowest flexural strain values emerged.

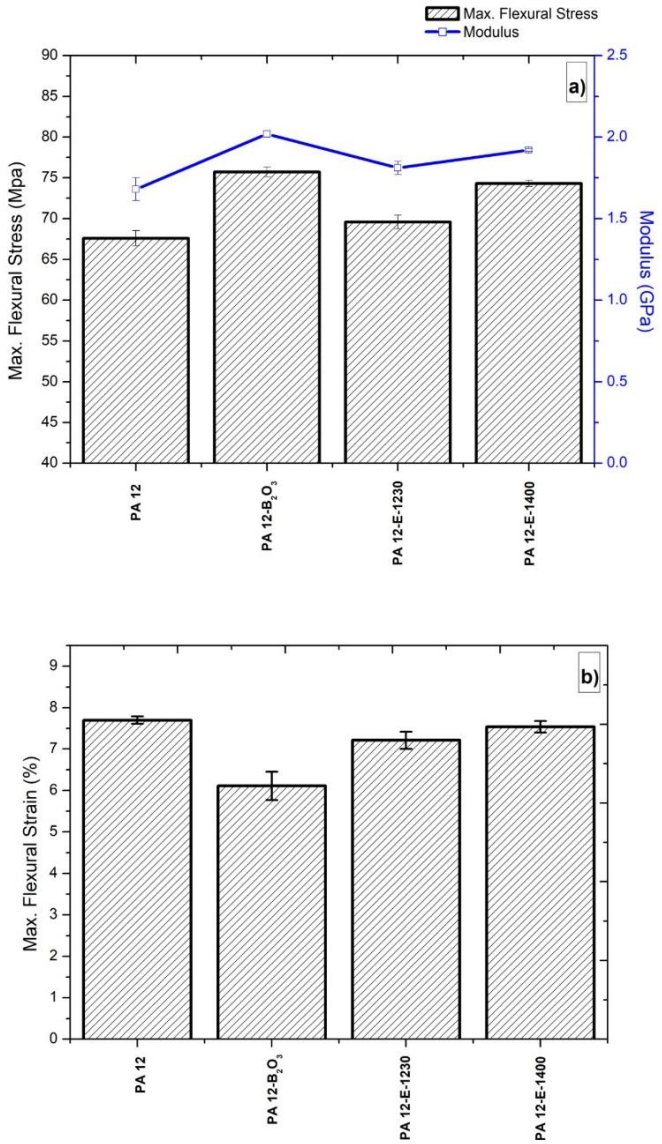

Figure 3.27 : Flexural test results of a) PA 12-B_2O_3, b) PA 12-E-1230, c) PA 12-E-1400 composite structures.

Charpy impact test results (Figure 3.28) reveal composite materials' mechanical behavior and toughness properties under sudden load. Reinforcement of PA 12 material generally caused embrittlement and reduced impact energy values. Especially with the use of B_2O_3, which has high hardness, strength and brittleness, the tensile and bending strength has increased, as mentioned before. However, the increase in strength values decreased the ductility of the material and caused a significant decrease in the impact strength value. Besides, similar impact strength values with were obtained in the use of E-1230 and E-1400.

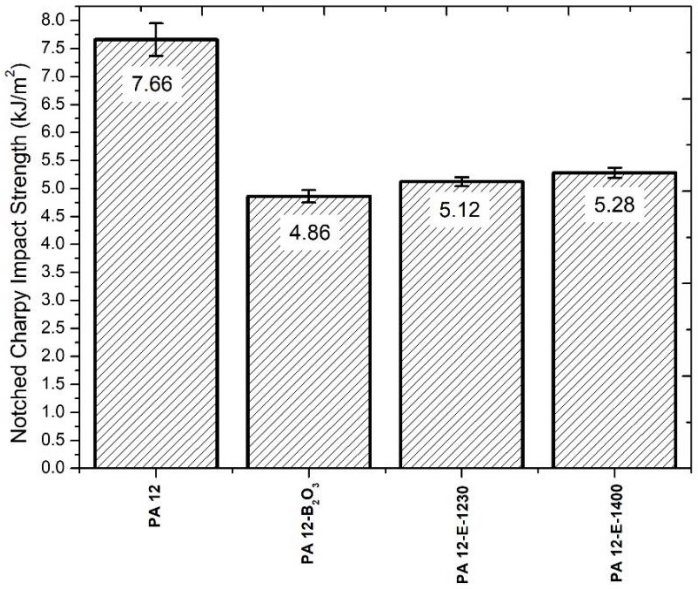

Figure 3.28 : Charpy impact test results of a) PA 12-B_2O_3, b) PA 12-E-1230, c) PA 12-E-1400 composite structures.

However, Figure 3.29 shows density measurements of PA 12 and PA 12 composite structures. The density values of the produced composite materials and the PA 12 matrix material were obtained in similar value ranges when the standard deviation values were taken into account.

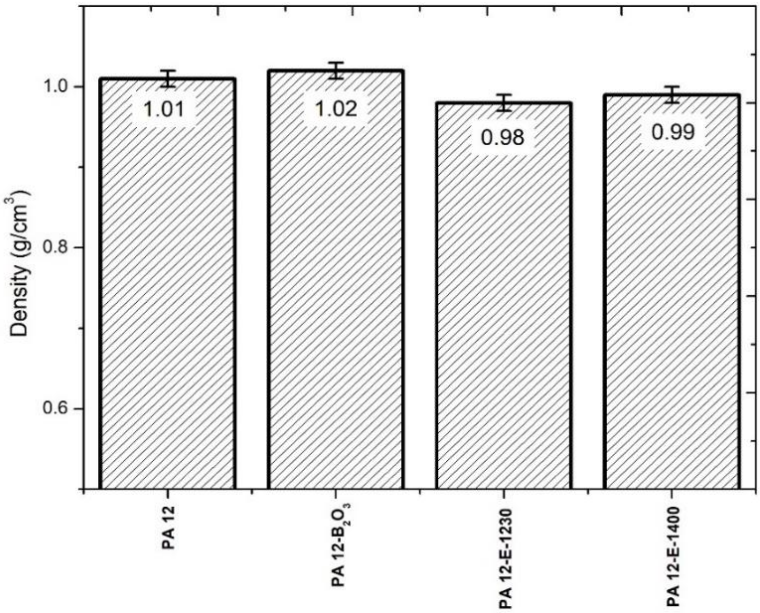

Figure 3.29 : Density measurements of a) PA 12-B_2O_3, b) PA 12-E-1230, c) PA 12-E-1400 composite structures.

3.4.2.2 SEM observations of sintered parts

The following figure demonstrates B_2O_3, Exolit 1230, and Exolit 1400 composite structures. According to Figure 3.30, it can be inferred that all additive types were homogeneously dispersed in the polymer matrix.

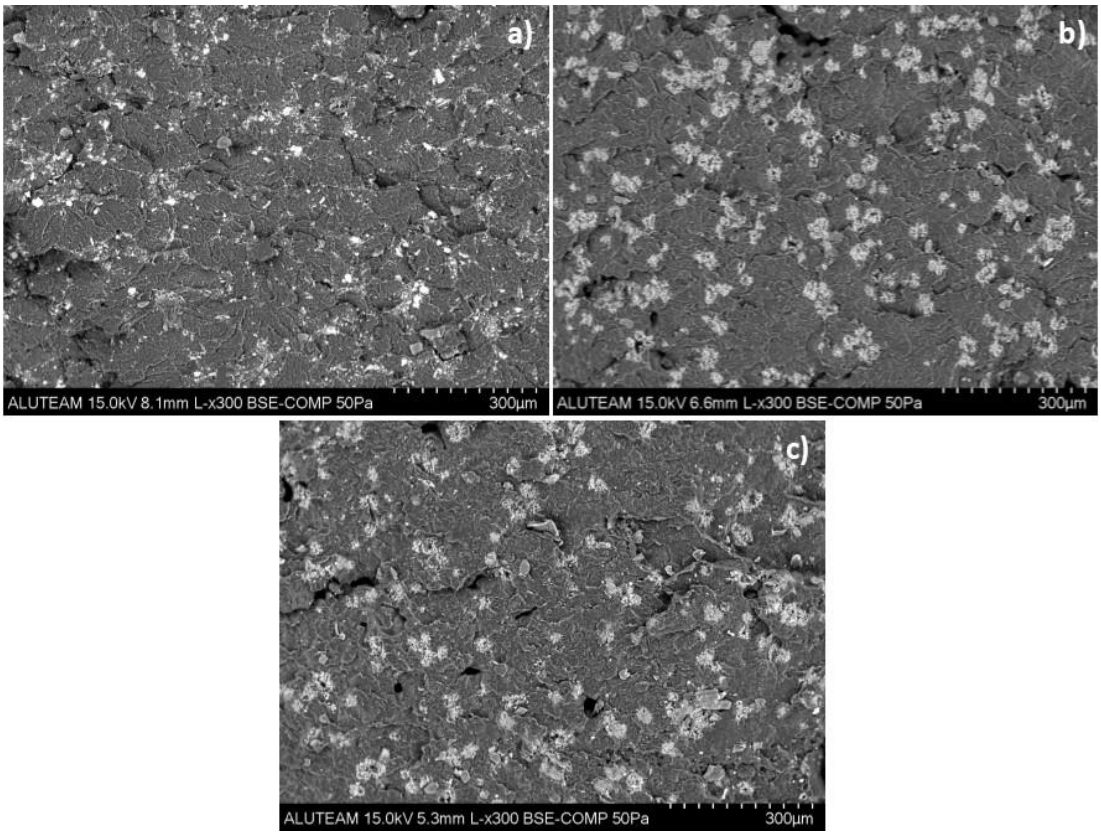

Figure 3.30 : SEM images of a) PA 12-B_2O_3, b) PA 12-E-1230, c) PA 12-E-1400 composite structures.

3.4.2.3 Flame retardancy test results of sintered parts

The flame retardancy features of polymer composites that were produced by SLS, and PA 12 itself, analyzed with LOI and UL-94 tests. Table 3.6 shows the FR test results of unfilled PA 12 and PA 12 composite structures. Unfilled PA 12 showed HB of UL-94 rating, which is Horizontal Burning and unacceptable for especially aerospace or electrical engineering applications. With the addition of B_2O_3, Exolit 1230, and Exolit 1400, this rate reached to V-2 level. According to oxygen index test results, it can be said that a small amount of increase by the addition of B_2O_3. With the Exolit additions, the values were decreased to around 21 %.

Table 3.6 : Flame retardancy test results of PA 12 and PA 12 composites.

Material	Flame Retardancy Class (UL 94)	Limited Oxygen Index (LOI %) (ISO 4589-2)
PA 12	HB	23.5
PA 12-B_2O_3	V-2	24.5
PA 12-E-1230	V-2	21.0
PA 12-E-1400	V-2	21.5

4. CONCLUSION

In the first part of the study, the effects of the increasing amount (10%, 15%, 20%) of one type of Hollow Glass Microsphere (HGM) on PA 12 polymer matrix structure were investigated. The main aim of this part was to obtain decreased density values without compromising much the stability and properties of SLS-produced parts. According to the performed test results, while the maximum tensile and flexural strain values decrease by the addition of HGM; Modulus, and stiffness results are developing, the density is reducing, and maximum tensile and flexural stress results are slightly changing. When the density measurement results and stiffness values were evaluated, PA12-20HGM (20% HGM addition) composite has been chosen as the optimized mixture in this study.

The second part of the research analyzed the effects of different types of hollow featured additives in PA 12 matrix. This part of the study aims to achieve density reduction by adding hollow glass additives in micron size and comparing the same amount (20%) and various types of hollow featured additives' effects on PA 12 polymer composites. As a result of thermal analysis it can be said that the addition of different types of hollow featured additives, polymer composite mixtures exhibited different crystallization temperatures, which also affects the LS process parameters as well. According to mechanical test results, higher tensile and flexural stress results and modulus values were obtained with PA 12-20HGS60 and PA 12-20HGM composites. However, it can be concluded that regarding to performed charpy impact tests, the spherical and rod-shaped particles were used together in the polyamide matrix, high impact values were achieved because of the increased absorbed energy. Nevertheless, the average particle size value at 20-30 MPa and high crush strength values of HGMs exhibited stiffer polymer composites structures.

The third part of the work was about the influence of energy density and filler types on PA 12 with two types of Cu fillers (dendritic and spherical forms) at 15 wt. % was experimented and compared to unfilled PA 12. In the thermal analysis of powder mixtures, Cu-filled samples had higher crystallization rates than unfilled PA 12. Also, higher building chamber temperature and Energy Density (ED) necessity were

determined for Cu-filled sample processing by SLS. On the other hand, as a result of DMA tests, higher transition temperatures and modulus values were obtained by adding spherical and dendritic copper additives. As flexural test examinations, it can be said that spherical Cu-filled samples had significantly higher flexural properties. On the other hand, with Cu metal fillers addition, the impact values were decreased. An observation had also been done according to the electrical conductivity of Cu-filled sintered parts. Higher conductivities were obtained with spherical Cu-filled samples, and conductivity values increased with increasing EDs.

In the final part of the research, developing the flame retardancy properties of PA 12 was researched. While the addition of different types of fire retardant fillers to PA 12 polymer matrix HB level of UL-94 result of unfilled PA 12, this value reached to V-2. For PA 12-B_2O_3, PA 12-E-1230, and PA 12-E-1400 composite structures, level of UL-94 result abtained as V-2. According to oxygen index test results, it can be said that a small amount of increase by the addition of B_2O_3. With the Exolit additions, the values were decreased to around 21 %.

In conclusion, it can be said that the addition of hollow featured microsphere additives to PA 12 polymer matrix can be suggested as an alternative material for aerospace and automotive industries for weight reduction of final structures. Besides, it can be concluded that flame retardancy properties could be improved by halogen-free fire retardant filler addition to PA 12 polymer matrix. As a future research perspective, the weight reduction and flame retardancy features would be more enhanced by these additions used together. Furthermore, using different types of additives, various types of composite materials could be created by the SLS method.

REFERENCES

[1] **Seo, D. C., Lee, J. J.** (1995). Effect of embedded optical fiber sensors on transverse crack spacing of smart composite structures. *Composite Structures*, *32*, 51-58. doi: 10.1016/0263-8223(95)00039-9.

[2]**Additive manufacturing.** Access date: 24 August 2021, https://www.dau.edu/library/defense-atl/p/Defense-ATandL-November December_2016

[3] **Noorani, R.** (2017). *3D Printing: Technology, Applications, and Selection*. Florida, CRC Press.

[4] **Ngo, T. D., Kashani, A., Imbalzano, G., Nguyen, K. T. Q., Hui, D.** (2018). Additive manufacturing (3D printing): A review of materials, methods, applications and challenges. *Composites Part B: Engineering*, *143*, 172-196. doi: 10.1016/j.compositesb.2018.02.012

[5] **Schmid, M.** (2018). *Laser Sintering with Plastics: Technology, Processes and Materials*. Carl Hanser Verlag.

[6] **Sun, S., Brandt, M., Easton, M.** (2017). Laser Additive Manufacturing: Materials, Design, Technologies, and Applications. *Powder bed fusion processes: An overview*. *Laser Additive Manufacturing: Materials, Design, Technologies, and Applications* (Vol 1, pp. 55-77). Retrieved from https://www.sciencedirect.com/science/article/pii/B9780081004333000026

[7] **Schmid, M., Wegener, K.** (2016). Additive Manufacturing: Polymers applicable for laser sintering (LS). *Procedia Engineering*, *149*, 457-464. doi: 10.1016/j.proeng.2016.06.692

[8] **Gan, X., Fei, G., Wang, J., Wang, Z., Lavorgna, M., Xia, H.** (2020). Structure and Properties of Additive Manufactured Polymer Components. *Powder quality and electrical conductivity of selective laser sintered polymer composite components* (Vol 2, pp. 149-185). Retrieved from https://www.sciencedirect.com/science/article/pii/B9780128195352000065

[9] **Gibson, I., Rosen, D., Stucker, B.** (2015). Additive Manufacturing Technologies. *Directed energy deposition processes*. (pp. 19–39).

[10] **Koo, J. H., Ortiz, R., Ong, B., Wu, H.** (2017). Laser Additive Manufacturing: Materials, Design, Technologies, and Applications. *Polymer nanocomposites for laser additive manufacturing* (pp. 205-235). Retrieved from

https://www.sciencedirect.com/science/article/pii/B9780081004333000087

[11] **Rashid, A. A., Khan, S. A., Al-Ghamdi, S. G., Koç, M.** (2021) Additive Manufacturing of Polymer Nanocomposites: Needs and challenges in materials, processes, and applications. *Journal of Materials Research and Technology*, *14*, 910-941. doi: 10.1016/j.jmrt.2021.07.016

[12] **Singh, S., Prakash, C., Ramakrishna, S.** (2020). Additive Manufacturing. *Polymer-Based Additive Manufacturing System* (pp. 19-44). Retrieved from https://www.worldscientific.com/doi/abs/10.1142/9789811224829_0001

[13] **Wortberg, J., Witt, G., Mielicki, C., Wegner, A., Gronhoff, B.** (2012). Prediction of PA12 melt viscosity in Laser Sintering by a Time and Temperature dependent rheological model. *Rapid Technology*, *2012* (9).

[14] **Polymer 3D printing market to generate $11.7 billion in 2020.** Access date: 26 August 2021: https://www.3dnatives.com/en/polymer-3d-printing-market-2020-040320204/#!

[15] **Wegner, A., Mielicki, C., Grimm, T., Gronhoff, B., Witt, G., Wortberf, J.** (2014). Determination of robust material qualities and processing conditions for Laser sintering of Polyamide 12. *Polymer Engineering and Science*, *54*, 1540-1554. doi: 10.1002/pen.23696

[16] **Gebhardt, A.** (2011). *Understanding Additive Manufacturing*. München, Hanser.

[17] **Stansbury J. W., Idacavage, M. J.** (2016). 3D printing with polymers: Challenges among expanding options and opportunities. *Dental Materials*, *32*, 54-64. doi: 10.1016/j.dental.2015.09.018

[18] **Schmidt, V., Belegratis, M. R.** (2013). *Laser Technology in Biomimetics*. Springer retrieved from https://link.springer.com/book/10.1007%2F978-3-642-41341-4

[19] **BSI (2017).** *Additive manufacturing: General principles*. Retrieved from https://standardsdevelopment.bsigroup.com/committees/50226095

[20] **Forster, A. M.** (2015). *Materials Testing Standards for Additive Manufacturing of Polymer Materials*, National Institutes of Standards and Technology.

[21] **Dizon, J. R. C., Espera, A. H., Chen, Q., Advincula, R. C.** (2018). Mechanical characterization of 3D-printed polymers. *Additive Manufacturing*, *20*, 44-67. doi: 10.1016/j.addma.2017.12.002

[22] **Goodridge, R. D., Shofner, M. L., Hague, R. J. M., McClelland, M., Schlea, M. R., Johnson, R. B., Tuck, C. J.** (2011). Processing of a Polyamide-12/carbon nanofibre composite by laser sintering. *Polymer Testing*, *30*, 94–100. doi: 10.1016/j.polymertesting.2010.10.011

[23] **Greiner, S., Wudy, K., Lanzl, L., Drummer, D.** (2017). Selective laser sintering of polymer blends: Bulk properties and process behavior. *Polymer Testing, 64,* 136-144. doi: 10.1016/j.polymertesting.2017.09.039

[24] **Cruz, P., Shoemake, E. D., Adam, P., Leachman, J.** (2015). Tensile strengths of polyamide based 3D printed polymers in liquid nitrogen. *IOP Conference Series: Materials Science and Engineering, 102,* 012020.

[25] **Negi, S., Sharma, R. K., Dhiman, S.** (2015). Experimental investigation of sls process for flexural strength improvement of PA-3200GF parts. *Materials and Manufacturing Processes, 30,* 644-653. doi: 10.1080/10426914.2014.994750.

[26] **Wohlers Report** (2020). 3D Printing and Additive Manufacturing State of the Industry. Access date: 26 August 2021 https://wohlersassociates.com/2020report.htm

[27] **Özbay, B., Serhatlı, E.** (2020), Processing and characterization of hollow glass-filled Polyamide 12 composites by Selective Laser Sintering method. *Materials Technology,* 1–11. doi:10.1080/10667857.2020.1824149

[28] **Yuan, S., Shen, F., Chua, C. K., Zhou, K.** (2019). Polymeric composites for powder-based additive manufacturing: Materials and applications. *Progress in Polymer Science, 91,* 141-168. doi: 10.1016/j.progpolymsci.2018.11.001

[29] **Bai, J., Goodridge, R. D., Hague, R.J. M., Song, M.** (2013). Improving the mechanical properties of Laser-sintered Polyamide 12 through incorporation of carbon nanotubes. *Polymer Engineering and Science, 53,* 1937-1946. doi: 10.1002/pen.23459

[30] **Goodridge, R. D., Tuck, C. J., Hague, R. J. M.** (2012). Laser sintering of polyamides and other polymers. *Progress in Materials Science, 57,* 229-267. doi:10.1016/j.pmatsci.2011.04.001

[31] **Ünal D.** (2020). *Development of in-situ thermal monitoring system for selective laser sintering to evaluate nesting design*. (MSc thesis). Retrieved from https://research.sabanciuniv.edu/41221/1/10352618_Unal_Deha.pdf

[32] **Palmer, R. J.** (2005). *Encyclopedia of Chemical Technology*. Wiley–Blackwell.

[33] **Schmid, M., Kleijnen, R., Vetterli, M., Wegener, K.** (2017). Influence of the origin of polyamide 12 powder on the laser sintering process and laser sintered parts. *Applied Sciences, 7,* 462. doi: 10.3390/app7050462

[34] **Mousa, A. A.** (2014), The effects of content and surface modification of filler on the mechanical properties of selective laser sintered polyamide12 composites. *Jordan Journal of Mechanical and Industrial Engineering, 8,* 265-274.

[35] **Goh, G. D., Yap, Y. L., Agarwala, S., Yeong, W. Y.** (2019). Recent progress in additive manufacturing of fiber reinforced polymer composite.

Advanced Materials Technologies, 4, 1800271. doi: 10.1002/admt.201800271

[36] **Salmoria, G. V., Leite, J. L., Vieira, L. F., Pires, A. T. N., Roesler, C. R. M.** (2012). Mechanical properties of PA6/PA12 blend specimens prepared by selective laser sintering. *Polymer Testing*, *31*, 411-416. doi: 10.1016/j.polymertesting.2011.12.006

[37] **Wudy, K., Lanzl, L., Drummer, D.** (2016). Selective laser sintering of filled polymer systems: Bulk properties and laser beam material interaction. *Physics Procedia*, *83*, 991-1002. doi: 10.1016/j.phpro.2016.08.104

[38] **Cano, A. J., Salazar, A., Rodríguez, J.** (2018). Effect of temperature on the fracture behavior of polyamide 12 and glass-filled polyamide 12 processed by selective laser sintering. *Engineering Fracture Mechanics*, *203*, 66-80. doi: 10.1016/j.engfracmech.2018.07.035

[39] **Chung, H., Das, S.** (2006). Processing and properties of glass bead particulate-filled functionally graded Nylon-11 composites produced by selective laser sintering. *Materials Science and Engineering A, 437*, 226–234. doi: 10.1016/j.msea.2006.07.112

[40] **Athreya, S. R., Kalaitzidou, K., Das, S.** (2010). Processing and characterization of a carbon black-filled electrically conductive Nylon-12 nanocomposite produced by selective laser sintering. *Materials Science and Engineering A, 527*, 2637-2642. doi: 10.1016/j.msea.2009.12.028

[41] **Athreya, S. R., Kalaitzidou, K., Das, S.** (2011). Mechanical and microstructural properties of Nylon-12/carbon black composites: Selective laser sintering versus melt compounding and injection molding. *Composites Science and Technology, 71*, 506-510. doi:10.1016/j.compscitech.2010.12.028

[42] **Jing, W., Hui, C., Qiong, W., Hongbo, L., Zhanjun, L.** (2017). Surface modification of carbon fibers and the selective laser sintering of modified carbon fiber/nylon 12 composite powder. *Materials and Design*, *116*, 253-260. doi: 10.1016/j.matdes.2016.12.037

[43] **Vahabi, H., Laoutid, F., Mehrpouya, M., Saeb, M. R., Dubois, P.** (2021). Flame retardant polymer materials: An update and the future for 3D printing developments. *Materials Science and Engineering Reports*, *144*, 100604. doi: 10.1016/j.mser.2020.100604

[44] **The flame retardants market.** Access date: 24 August 2021 https://www.flameretardants-online.com/flame-retardants/market

[45] **Batistella, M., Regazzi, A., Pucci, M. F., Lopex-Cuesta, J. M., Kadri, O., Bordeaux, D., Ayme, F.** (2020). Selective laser sintering of polyamide 12/flame retardant compositions, *Polymer Degradation and Stability*, *181*, 109318. doi: 10.1016/j.polymdegradstab.2020.109318

[46] **Schneider, K., Wudy, K., Drummer, D.** (2020). Flame-retardent polyamide powder for laser sintering: Powder characterization, processing behavior and component properties. *Polymers*, *12*, 1697. doi: 10.3390/polym12081697

[47]**PA 2200-Polyamide 12 TDS.** Access date: 24 August 2021 https://www.eos.info/en/additive-manufacturing/3d-.

[48] **Pilipovic, A., Drstvensek, I., Sercer, M.** (2014). Mathematical model for the selection of processing parameters in selective laser sintering of polymer products. *Advances in Mechanical Engineering, 2014* (1), 1-9. doi: 10.1155/2014/648562

[49] **Lanzl, L., Wudy, K., Greiner, S., Drummer, D.** (2019). Selective laser sintering of copper filled polyamide 12, *Polymer Composites*, *40*, 1801-1809. doi: 10.1002/pc.24940

[50**] Lanzl, L., Wudy, K., Drummer, D.** (2020). The effect of short glass fibers on the process behavior of polyamide 12 during selective laser beam melting. *Polymer Testing*, *83*, 106313. doi:10.1016/j.polymertesting.2019.106313

[51] **ISO** (2012). *Plastics-determination of tensile propertiespart 2: test conditions for molding and extrusion plastics* (ISO Standard No. 527–2:2012). Retrieved from: https://www.iso.org/standard/56046.html

[52] **ISO** (2019). *Plastics-determination of flexural properties* (ISO Standard No. 178:2019). Retrieved from: https://www.iso.org/standard/70513.html

[53] **ISO** (2010). *Plastics-determination of charpy impact properties-part 1: non-instrumented impact test* (ISO Standard No. ISO 179–1:2010). Retrieved from https://www.iso.org/stan%0Adard/44852.html

[54] **ASTM** (2013). *Standard Test Method for Plastics: Dynamic Mechanical Properties : In Torsion* (ASTM D5279-13).

[55] **UL 94** (2013). *Tests for Flammability of Plastic Materials for Parts in Devices and Appliances*. Retrieved from https://standardscatalog.ul.com/ProductDetail.aspx?productId=UL94

[56] **ASTM** (2019). *Standard Test Method for Measuring the Minimum Oxygen Concentration to Support Candle-Like Combustion of Plastics (Oxygen Index)* (ASTM D2863-19) Retrieved from file:///D:/flame üretim/STANDARD LOI-UL94/UL 94-D3801.37830.pdf

[57] **Majewski, C. E, Zarringhalam, H., Hopkinson, N.** (2008). Effects of degree of particle melt and crystallinity in SLS Nylon-12 parts. *Proceedings of the Institution of Mechanical Engineers, Part B: Journal of Engineering Manufacture*, *222*, 1055-1064.

[58] **Craft, G. M.** (2018). *Characterization of nylon-12 in a novel additive manufacturing technology, and the rheological and spectroscopic*

analysis of peg-starch matrix interactions. (Doctoral dissertation). Retrieved from https://digitalcommons.usf.edu/etd/7137/

[59] **ASTM** (1997). *Standard Test Method for Sheet Resistance Uniformity Evaluation by In-Line Four- Point Probe with the Dual-Configuration Procedure*. Retrieved from https://www.astm.org/Standards/F1529.htm

[60] **Ummartyotin, S., Juntaro, J., Wu. C., Sain, M., Manuspiya, H.** (2001). Deposition of PEDOT: PSS nanoparticles as a conductive microlayer anode in OLEDs device by desktop inkjet printer. *Journal of Nanomaterials*, *26*, 1-7. Doi: 10.1155/2011/606714.

CURRICULUM VITAE

Name Surname : Burçin Özbay

EDUCATION :

- **B.Sc.** **:** 2013, Yildiz Technical University, Faculty of Chemical and Metallurgical Engineering, Metallurgical and Materials Engineering
- **M.Sc.** **:** 2015, Yildiz Technical University, Graduate School of Natural and Applied Sciences, Materials Science and Engineering
- **M.Sc. (Erasmus +)** **:** 2015, Technical University of Clausthal (TU Clausthal) Institute of Polymer Materials and Plastics Engineering

PROFESSIONAL EXPERIENCE AND REWARDS:

- 2018-Present-Research Engineer - Fatih Sultan Mehmet Vakif University, Aluminum Test, Education, and Research Center – Istanbul-Turkey
- 2015-2017-Research and Development Engineer – PolyOne Corporation – Istanbul-Turkey
- 2014-2015-Assistant Research and Development Engineer – MIR AR-GE – Istanbul-Turkey

PUBLICATIONS, PRESENTATIONS AND PATENTS ON THE THESIS:

- **Özbay, B.,** Bekem, A., Serhatlı, İ., E., Öztürk, S., Bulduk, M. E. 2021. Effects of copper fillers on mechanical and electrical properties of selective laser sintered PA 12-Cu composites, *Materials Technology: Advanced Performance Materials*, DOI: 10.1080/10667857.2021.1964203
- **Özbay, B.,** Serhatlı, İ., E., Bulduk, M., E., 2021. SLS Manufacturing and Characterization of Lightweight PA 12 Polymer Composites with Different Hollow Microsphere Additives. Journal of Materials Engineering and Performance (under review, revision has been submitted).
- **Özbay, B.,** Serhatlı, İ., E. 2020. Processing and Characterization of Hollow Glass-Filled Polyamide 12 Composites by Selective Laser Sintering Method,

Materials Technology: Advanced Performance Materials, DOI: 10.1080/10667857.2020.1824149

- **Özbay, B.,** Serhatlı, İ., E., Bulduk M. E. 2021: Hollow Glass Microsphere And Glass Bead-Polyamide 12 Composites Production By Selective Laser Sintering Method, IMMC'2021 International Metallurgy & Materials Congress, June 10-12, 2021 İstanbul, Turkey.
- **Özbay, B.,** Serhatlı, İ., E. 2020: Hollow Ceramic And Glass Microsphere Filled Polyamide 12 Composites Production By SLS Additive Manufacturing Method, SPE-ACCE (Automotive Composites Conference), September 9-11, 2020 Michigan, US.
- **Özbay, B.,** Serhatlı, İ., E., Bulduk, M. E. 2019: Manufacturing and Characterization of Filled Polyamide 12 Composite Structure By Selective Laser Sintering Method. 5th Edition of International Conference on Polymer Science and Technology, June 10-11, 2019 Berlin, Germany.

OTHER PUBLICATIONS, PRESENTATIONS AND PATENTS:

- **Özbay, B.,** Bekem, A., Bulduk, M. E. 2021: Effect Of Dendritic Copper Powder Addition To Polyamide 12 In Selective Laser Sintering, *Journal Of The Faculty Of Engineering And Architecture Of Gazi University*, 36 (1), 421-431.
- **Özbay, B.,** Bekem, A., Ünal, A. 2020: Manufacturing of Hybrid Yarn Thermoplastic Composites by the Method of Filament Winding, *Gazi University Journal Of Science*, 33 (1), 214-227.
- Özer, G., **Özbay B.,** Öter, Z. Ç., Tarakçı, G., Yılmaz, M. S., Bulduk, M.E., Koç, E., Acar, S., Güler, K. A. 2020. Investigation Of The Surface Quality And Dimensional Accuracy Of Polymer Patterns Produced By Selective Laser Sintering (SLS) Method For Investment Casting (IC), International *Journal of Cast Metals Research*, doi.org/10.1080/13640461.2020.1773053.
- **Özbay, B.,** Özer, G., Bulduk, M. E., Tarakçı, G., Öter, Z. Ç., Koç, E. 2019: Productıon of PRIMECAST® Polystyrene by Selective Laser Sintering (SLS) Method and Development of Surface Roughness of Sintered Parts, Additive Manufacturing Conference (AMC TURKEY), September 17-18, 2019 İstanbul, Turkey.